OPTIMAL MATERIAL MODEL FOR ANALYSIS OF WOOD GUARDRAIL

A Thesis

by

NATALY DE LA FUENTE

Submitted to the Office of Graduate and Professional Studies of
Texas A&M University
in partial fulfillment of the requirements for the degree of

MASTER OF SCIENCE

Chair of Committee,	Gary T. Fry
Committee Members,	Nasir G. Gharaibeh
	Alan B. Palazzolo
Head of Department,	Robin Autenrieth

May 2018

Major Subject: Civil Engineering

ABSTRACT

The overall performance of guardrail systems is mostly dependent on the strength of the wood posts. Therefore, developing an accurate model of wood post components of guardrail systems is essential. Wood posts are among the most common materials currently used in highway construction. Accurately simulating the breakaway characteristics of wood material posts is necessary for design. In this study, different material models are evaluated to determine their accuracy of representing the wood post behavior including, the failure behaviors of southern yellow pine wood. The material models are evaluated for a controlled release terminal (CRT) post and a standard guardrail post being impacted by a pendulum. Finite-element software LS-Dyna is one method that can be used to analyze the failure behavior. A description is provided of the development of the material models for the CRT and standard wood post. The simulation results are compared with data from tests performed by Texas A&M Transportation Institute (TTI) to find the material model which best matches the experimental data. The accuracy of the results was based on a qualitative comparison. This research shows that material model - 143 wood pine responded with more accuracy compared to the other material models.

ACKNOWLEDGEMENTS

I would like to thank my committee chair, Dr. Gary Fry for his guidance and support throughout the course of this research. Special thanks Dr. Nasir G. Gharaibeh and Dr. Alan B. Palazzolo for serving as my committee members of this thesis committee. I would also like to express my appreciation to Dr. Akram Abu-Odeh for his support and help through my master's degree. Thanks also to my friends and colleagues, especially Melissa Martinez and Maryam Tavakoli. The department faculty and staff for making my time at Texas A&M University a great experience. To the Texas A&M Transportation Institute and Texas A&M Supercomputing Facility for their generous allocation of facilities and computational resources.

Finally, thanks to my family, especially, my mother for giving me infinite support and love and my father for giving me the motivation and encouragement to accomplish all my goals.

CONTRIBUTORS AND FUNDING SOURCES

Contributors

This work was supervised by a thesis committee consisting of advisor Dr. Fry, Dr. Gharaibeh of the Zachary Department of Civil Engineering and Dr. Palazzolo of the Department of Mechanical Engineering. All work for the thesis was under the advisement of Dr. Gary Fry and Dr. Akram Abu-Odeh from Texas A&M Transportation Institute.

The pendulum field test results in Chapter 2 and data in Chapter 3 were provided by Texas A&M Transportation Institute (TTI). All other work conducted for the thesis was completed by Nataly de la Fuente independently.

Funding Sources

This work was made possible in part by the Texas Department of Transportation under Project Number 0-6913-16.

TABLE OF CONTENTS

Page

ABSTRACT ii

ACKNOWLEDGEMENTS iii

CONTRIBUTORS AND FUNDING SOURCES iv

TABLE OF CONTENTS v

LIST OF FIGURES vii

LIST OF TABLES ix

1. INTRODUCTION 1

1.1. Nature of Wood 2
1.2. Structure of Wood 4
1.3. Wood Properties 5
1.3.1. Mechanical Properties of Wood 6
1.3.2. Physical Properties of Wood 8

2. PROCEDURES 12

2.1. Pendulum Tests 13
2.2. Finite Elements Simulation of Posts and Pendulum 14
2.3. Material Models 15
2.3.1. Material Model 123 Modified Piecewise Linear Plasticity 16
2.3.2. Material Model 143 Wood 16
2.3.3. Material Model 143 wood pine 20

3. RESULTS 21

3.1. Controlled Release Terminal Post – Strong Axis 21
3.1.1. Material Model 123 Modified Piecewise Linear Plasticity 22
3.1.2. Material Model 143 Wood 22
3.1.3. Material Model 143 Wood Pine 23
3.2. Controlled Release Terminal Post – Weak Axis 23
3.2.1. Material Model 123 Modified Piecewise Linear Plasticity 23
3.2.2. Material Model 143 Wood 24
3.2.3. Material Model 143 Wood Pine 24
3.3. Standard Timber Post – Strong Axis 24
3.3.1. Material Model 123 Modified Piecewise Linear Plasticity 25

3.3.2. Material Model 143 Wood 25
3.3.3. Material Model 143 Wood Pine 25
3.4. Standard Timber Post – Weak Axis 26
3.4.1. Material Model 123 Modified Piecewise Linear Plasticity 26
3.4.2. Material Model 143 Wood 27
3.4.3. Material Model 143 Wood Pine 27

4. DISCUSSION 28

5. CONCLUSION 30

REFERENCES 31

APPENDIX A FIGURES 33

APPENDIX B TABLES 63

LIST OF FIGURES

Page

Figure 1. Southern Yellow Pine Growth Rings (adapted from Bruce Hoadley)[3] 33

Figure 2. Three Principal Axes of Wood (adapted from Bushchow)[13] 33

Figure 3. Knot Defect Found in a Board that has Been Cut Away From a Tree. (modified from Murray) [5] 34

Figure 4. Pendulum Design Model 34

Figure 5. Wood Posts 35

Figure 6. Longitudinal Acceleration for CRT Post in Strong Axis – Field Tests 35

Figure 7. Sequential Images of CRT Post – Strong Axis (Material 123) 36

Figure 8. Longitudinal Acceleration for CRT Post in Strong Axis – Material 123 37

Figure 9. Sequential Images of CRT Post - Strong Axis (143 Wood) 38

Figure 10. Longitudinal Acceleration for CRT Post in Strong Axis – Material 143 Wood 39

Figure 11. Sequential Images of CRT Post – Strong Axis (143 Wood Pine) 40

Figure 12. Longitudinal Acceleration for CRT Post in Strong Axis – Material 143 Wood Pine . 41

Figure 13. Longitudinal Acceleration for CRT Post in Weak Axis – Field Tests 42

Figure 14. Sequential Images of CRT Post – Weak Axis (Material 123) 43

Figure 15. Longitudinal Acceleration for CRT Post in Weak Axis – Material 123 44

Figure 16. Sequential Images of CRT Post - Weak Axis (143 Wood) 45

Figure 17. Longitudinal Acceleration for CRT Post in Weak Axis – Material 143 Wood 46

Figure 18. Sequential Images of CRT Post – Weak Axis (143 Wood Pine) 47

Figure 19. Longitudinal Acceleration for CRT Post in Weak Axis – Material 143 Wood Pine .. 48

Figure 20. Longitudinal Acceleration for Standard Post in Strong Axis – Field Test 49

Figure 21. Sequential Images of Standard Post – Strong Axis (Material 123) 50
Figure 22. Longitudinal Acceleration for Standard Post in Strong Axis – Material 123 51
Figure 23. Sequential Images of Standard Post - Strong Axis (143 Wood) 52
Figure 24. Longitudinal Acceleration for Standard Post in Strong Axis – Material 143 Wood... 53
Figure 25. Sequential Images of Standard Post - Strong Axis (143 Wood Pine) 54
Figure 26. Longitudinal Acceleration for Standard Post in Strong Axis – Material 143 Wood Pine 55
Figure 27. Longitudinal Acceleration for Standard Post in Weak Axis – Field Tests..... 56
Figure 28. Sequential Images of Standard Post - Weak Axis (Material 123)..... 57
Figure 29. Longitudinal Acceleration for Standard Post in Weak Axis – Material 123..... 58
Figure 30. Sequential Images of Standard Post - Weak Axis (143 Wood)..... 59
Figure 31. Longitudinal Acceleration for Standard Post in Weak Axis – Material 143 Wood.... 60
Figure 32. Sequential Images of Standard Post – Weak Axis (143 Wood Pine)..... 61
Figure 33. Longitudinal Acceleration for Standard Post in Weak Axis – Material 143 Wood Pine 62

LIST OF TABLES

Page

Table 1. Material Model 123 - Parameters for Southern Yellow Pine Wood..... 63

Table 2. Material Model 143 Wood - Parameters for CRT Post in the Strong Axis..... 64

Table 3. Material Model 143 Wood - Parameters for CRT Post in the Weak Axis 65

Table 4. Material Model 143 Wood - Parameters for Standard Post in the Strong Axis..... 66

Table 5. Material Model 143 Wood - Parameters for Standard Post in the Weak Axis..... 67

Table 6. Material Model 143 Woodpine - Parameters for Southern Yellow Pine Wood..... 68

Table 7. Parameters for Southern Yellow Pine with Moisture Content 1%..... 69

Table 8. Parameters for Southern Yellow Pine with Moisture Content 7%..... 70

Table 9. Parameters for Southern Yellow Pine with Moisture Content 12%..... 71

Table 10. Parameters for Southern Yellow Pine with Moisture Content 23%, at Saturation..... 72

1. INTRODUCTION

Timber posts are widely used in guardrail systems because they are inexpensive and easy to install. Also their capacity to absorb considerable load without failing makes them ideal for dissipating the energy associated with a vehicle impact. There are two popular methods that are utilized to analyze a wood post component: full scale crash testing and finite element simulations. Finite element (FE) analysis has become a fundamental part of the analysis for design. FE programs have been adopted by many industries as part of their design process in order to minimize the cost and maximize the efficiency of the structure. Advantages from using this method are cost and time, but the main advantage is the ability to predict the impact damages that are barely visible and hard to identify [1]. It allows the analyst to have more control over the material and impact conditions and provide detail information about the mechanics of the impact. This method of modeling and simulation allows a deeper scientific knowledge of how the wood material behaves, since the results provide integral information about the material.

In this study, the timber post model is constructed and analyzed using LS-DYNA. The geometrical modeling of the elements is an easy task in preprocessor technology; however, characterizing the material behavior of wood is the challenge of modeling. The properties of the newly created structure can be modified by the combination of materials with distinct properties. Simulating the material and physical behavior of wood posts has been a concern when developing models of guardrail systems [2]. Wood is an anisotropic fibrous material that exhibits a complex mode of failure in bending, due primarily to the difference in tensile and compressive strength of wood. It is a versatile material with a wide range of physical and mechanical properties and is also a renewable resource with an exceptional strength-to-weight ratio. Modeling the behavior of wood would be difficult with the existing anisotropic material

due to limitations in the models' failure criteria. However, there are simple isotropic material models available in the software program that is capable of simulating the response and fracture of the wood post.

The failure modes of each guardrail posts are observed, in which the longitudinal fibers of the post progressively fail in tension. This is due to the bending on the impact face of the post. This can be simulated with the material models that depict which model is accurate to resemble the response on the actual behavior of a wood post. Before going into details of simulating the material model of wood, it is helpful to have an understanding of wood. This includes the cellular structure of wood, its properties, species and factors that affect its failure behavior.

1.1. Nature of Wood

Wood comes from trees and, despite the diversity; all trees have certain common characteristics. All are vascular, perennial plants capable of secondary thickening, or adding yearly growth to previous growth [3]. Examining the structure of the entire tree as a living organism, will help one understand the grain direction, visualize a knot's internal structure based on its surface appearance, and anticipate which wood posts are susceptible to decay.

Understanding the cell structure of wood is the key to knowing what is happening within the wood post. The tree is made of an accumulation of countless cells. These cells are the basic structural unit of a plant material. Each cell consists of an outer cell wall surrounding an inner cell cavity [3]. Some cells have living protoplasm within, while others are nonliving cells that contain sap or even air space. Wood cells are typically elongated. The proportion of length to diameter of the cells varies widely on the cell types. The majority of wood is composed of longitudinal cells, whose axes are oriented vertically in the tree stem [3]. There are also groups of cells whose axes are horizontal, which extend radially outward from the pith and are called

rays. These rays are flattened ribbons of cells that vary in size according to the number of cells contained within them.

Cells of similar function are referred to as tissue, wood tissue or bark tissue. These two tissues are permanent tissues because once they are formed and matured; their cells retain their shape and size. The wood cells that are produced by a layer of cells between the bark and the wood is called the cambium. Full growth of the tree is the result of thickness growth produced by division of the cambium, a lateral meristem. The growth of trees is also affected by the soil and environmental conditions.

In the cambium, cells reproduce by dividing lengthwise. One of the cells becomes another cambial cell and the other cell either becomes a new bark cell or wood cell. The wall cell on the inside of the cambium elongates or enlarges or both. Once the cells have attained their ultimate size and shape, a secondary wall has formed. After this thickened wall is produced, it becomes the dominant layer of the cell forming a fixed cell size and shape for ever. This secondary wall is built mainly of cellulose long chain molecules that are strong and stable. These cellulosic structures are fortified by lignin, the material that characterizes woody plants.

During the last stages of the maturing process, most of the wood cells that were produced by the cambium become sapwood. The wood cells lose their living protoplasm and sap is left in them. In this newly formed sapwood, a small percentage of the cells, found in the rays, retain their living protoplasm and can assimilate and store food. Sapwood is the wood portion of the stem that involves sap conduction upward in the tree. The sapwood transforms into heartwood and in this transition, it is accompanied by the formation in the cell wall of material called extractives.

The activity of the cambium continues depending on the suitable environmental conditions and if the tree is healthy. The nature of wood cell formation is similarly cyclic, which results in visible growth layers. The increments of these growth layers are also called growth rings or annual rings. Growth rings are arranged around the central pith and they are what characterize wood. These rings are formed in association with yearly growth and vary in width as a characteristic of species and growing conditions. Rings formed during short or dry seasons are thinner than those formed when growing conditions are more favorable. Also rings formed in shady conditions are usually thinner than those formed by the same species in sunny conditions. It is commonly believed that the age of the tree may be determined by counting these rings. However this method can lead to errors. The reason being because abnormal environmental condition can cause a tree to produce multiple-growth increments or even prevent growth entirely for a period.

When there is visible contrast within a single growth ring, the first formed layer is known as earlywood and remainder is latewood. Figure 1 shows each growth ring in southern yellow pine. Each layer is distinct showing a light, soft layer of earlywood followed by a dark and dense layer of latewood. The contrast between earlywood and latewood predicts the difference in hardness of the wood. Latewood is sometimes used to judge the quality or strength of some species. Earlywood is weaker than latewood, because it shrinks less across the grain than latewood.

1.2. Structure of Wood

Wood is an example of an orthotropic and anisotropic material. Because of the arrangement of the layers of growth in the tree, as well as the vertical or horizontal orientation of the individual cells, it is appropriate to consider the structure of wood in three-dimensional terms [3]. Stiffness and strength are properties that vary as a function of orientation between the

longitudinal, tangential and radial directions. Figure 2 illustrates the three principal axes of wood. The longitudinal axis is parallel to the cylindrical trunk of the tree and also to the wood fibers. The tangential axis is perpendicular to the grain but tangent to the growth rings and the radial axis is normal to the growth rings. Both the tangential and radial axes are perpendicular to the grain. Most of the wood properties differ in each of the three axis directions. However, the difference between the radial and tangential axes is relatively minor when compared to differences between the radial or tangential axis and the longitudinal axis [4].

1.3. Wood Properties

Of all properties of wood, strength is the most important. It is often defined as the ability to resist the applied stress and the strength of the material is synonymous with the resistance of the material [3]. Wood strength varies significantly depending on the species, loading conditions, load duration and the environmental factors. The relationship between stress and strain is of primary concern when considering the strength of wood. The stress-strain relationships of wood in parallel tension, perpendicular tension, and shear are typically linear to brittle failure, while in parallel compression and perpendicular compression are typically nonlinear and ductile [5].

Density is an important indicator of strength in wood; it is the mass per unit volume at some specified condition. A dense wood usually shrinks and swells more and will present greater problems in drying. Because of volumetric shrinkage and swelling, the volume of wood may vary slightly with moisture content. Density is expressed as specific gravity, which is a dimensionless ratio of the density of a substance to the density of a standard substance. For many engineering applications, the basis for specific gravity is generally the oven dry weight and volume at moisture content of 12% [4]. Strength of wood may be affected by both mechanical

and physical properties. It is significant to understand how the mechanical and physical properties apply to the strength on a wood post.

1.3.1. Mechanical Properties of Wood

The mechanical properties of wood are the characteristics of a material in response to external applied forces. They include elastic properties, the characterization of resistance to deformation and distortion, and strength properties, the resistance to applied loads. These properties are given in terms of stress and strain and are obtained from laboratory tests of clear wood samples. In this study the mechanical properties where based on test provided by the Manual for LS-DYNA Wood Material Model 143.

1.3.1.1. Elastic Properties

Elastic properties are produced at low stress levels and are completely recoverable after the loads are removed, for a material with ideal elastic properties [3]. For wood it is not ideally elastic in that some of the deformation is not immediately recovered but over a period of time residual deformation is generally recovered. Although wood is usually assumed to behave as an elastic material for most engineering applications [4]. Since wood is orthotropic, the elastic properties of wood are characterized by nine independent constants. The nine independent constants are three moduli of elasticity or Young's modulus (E), three shear moduli (G), and three Poisson ratios (μ). Young's moduli are used to characterize strain in the orthotropic directions, and are usually determined from compression tests. Poisson ratio is when a member is loaded axially; the deformation perpendicular to the direction of loading is proportional to the deformation in the direction of loading. The elastic constants vary by species, moisture content, and temperature at which they are measured.

When using an isotropic material, the elastic properties are measured by the three elastic constants, modulus of elasticity, modulus of rigidity, and Poisson's ratio. The following equation shows the relationship of the three elastic constants:

$$\mu_{ij} = {E_k}/{G_{ij}} \quad (1)$$

Where *i, j* and *k* represent the three principal axes.

1.3.1.2. Strength Properties

Plastic deformation or failure occurs when wood is loaded to higher stress levels beyond the elastic range. Six strength properties that are commonly measured for design purposes include modulus of rupture, tension parallel and perpendicular to the grain, compression parallel and perpendicular to the grain, and shear parallel to the grain. In addition other measurements are sometimes required such as the energy absorption resistance, fatigue and/or hardness.

When loaded in tension parallel to the grain, wood is very strong in tension. Two different failure modes occur, the cell-to-cell slippage and cell wall failure. Slippage occurs where two adjacent cells slide past one another. Cell wall failure occurs when there is the involvement of rupture within the cell wall with little or no visible deformation prior to complete failure. In contrast, wood is weak when loaded in tension perpendicular to grain. These stresses act perpendicular to the cell lengths and create splitting or cleavage along the grain. Splitting and cleavage can have a significant effect on the structural integrity. The deformations are usually low prior to failure because of the geometry and structure of the cell wall cross-section [4].

When a compression load is applied parallel to grain, it produces stress that deforms wood cells along their longitudinal axis [4]. As stress continues to increase, the wood cells form visible wrinkles on the surface folded into S shapes. A larger deformation occurs from the internal

crushing of the complex cellular structure. When a compression load is applied perpendicular to grain, it produces stress that deforms the wood cells perpendicular to their length. The hollow cell cavities collapse and once there is no void space that exists, the wood is quite strong. When wood is used as a beam, it is exposed to compression stress on one surface and tensile stress on the other. This results in a shearing action where the parallel-to-grain shearing action is termed horizontal shear. However, when stress is applied perpendicular to the cell length in a plane parallel to grain, this action is termed rolling shear [4]. In rolling shear stresses, there is a tendency for wood cells to roll over one another.

Energy absorption is a function, and it has the ability of a material to quickly absorb and then dissipate energy through deformation. Wood is good candidate in this respect is a preferred material for shock loading. There are several parameters that are used to describe energy absorption; the parameters depend on the eventual criteria of failure that is being considered. The work to proportional limit, work to maximum load, and work to total failure describe the energy absorption of wood materials at progressively more severe failure criteria [4].The fatigue resistance of wood is sometimes important to consider. Wood is quite resistant to fatigue and at comparable stress levels, the fatigue strength of wood is often several times that of most metals. Hardness represents the resistance of wood to indentation and marring. Hardness is measured by force required to embed into the wood.

1.3.2. Physical Properties of Wood

The physical properties are the quantitative characteristics of wood and its behavior to external influences other than applied forces [4]. Many factors affect the strength of wood. These factors include moisture content, temperature, defects and species of wood. Being familiar with

the physical properties is important because they can significantly influence the performance and strength of wood.

Moisture content is a factor that affects the behavior of wood by affecting the measured stress-strain relationship. The moisture content of wood is defined as the weight of water in wood given as a percentage of oven dry weight. Moisture content is expressed in the following equation:

$$MC = \frac{moist\ weight - dry\ weight}{dry\ weight} \times 100\% \quad (2)$$

Water is required for the development and growth of trees. The moisture content of trees depends on the species and the type of wood and can range from approximately 25% to more 250% [4]. The strength of wood increases as moisture content decreases below the fiber saturation point, which is where the cell walls are fully saturated, but cell cavities are free of water. Wood is a material that absorbs moisture in a humid environment and loses moisture in a dry environment. Because of this, moisture content of wood is a function of atmospheric condition and depends on the relative humidity and temperature of the surrounding air.

Temperature will also affect the strength of the wood. This temperature effect depends on the moisture content of the wood and the surrounding environment. For instance, if dry wood is heated in dry air, the wood will expand. For ordinary conditions of wood containing more or less moisture, high heat temperatures have a drying effect which also causes shrinkage. The shrinkage completely obscures the expansion due to the heating [6]. In wet conditions of wood, high temperatures its strength may be reduced and for dry conditions the effect of cold increases the strength and stiffness of wood. As a result, as temperature decreases the strength in wood increases and as temperature rises, wood strength decreases

Another factor, defects in this case, refer to the irregularities or features affecting the strength of wood. Such defects are knots, checks, shakes and splits. Knots are the most common encountered defects that reduce strength, Figure 3. The reduction in strength depends on the knot size relative to the board size, the knot position, and the wood parallel tensile strength. It has an abnormal cell structure that runs at an angle to the surrounding grain direction. The area around the knot typically contains cross grain that result in severe strength reduction. The degree of weakening caused by knots is quite variable and unpredictable.

Checks are the separation of the wood and it normally occurs across or through the rings of annual growth. There are two types of checks, surface checks and end checks. Surface checks are failures that occur in the wood rays on the flat saw faces of the cut wood. These defects occur because of the drying stresses exceed the tensile strength of wood perpendicular to the grain, and they are caused by tension stresses that develop in the outer part of the post or boards as they dry around the still wet and swollen core. End checks occur because of moisture. The moisture moves faster in the longitudinal direction than in either transverse direction, causing the ends of the cut out post dry faster than the middle and stresses develop at the ends.

Shakes are a defined lengthwise separation of the wood along the tangential direction than can occur on the surface or through the wood that extends from one side to the opposite side of the wood. This defect usually occurs between or through the rings of annual growth. Shakes naturally occur in trees by the separation of latewood fibers, and are found that bacteria, tree wounds, age and environmental conditions are the cause of this defect [7]. The last defect are splits, which are also the separation of wood through the wood piece to the opposite surface due to the tearing apart of the wood cells. Splits are caused by drying or by growth stresses and can extend across one or more growth rings.

Moisture content and defects are two important factors that affect the strength property of wood, but the species of wood is another important factor that influences the strength of a wood post. There is a variety of wood species where they can be classified as either softwood or hardwood. Softwood and hardwood refer mainly to the kind of trees that produce the wood and not precisely to the hardness or softness of the woods themselves. Hardwood is angiosperm trees, which have relatively short cell that conduct water primarily through openings on their end walls. Softwood on the other hand is a gymnosperm tree, composed of long cells that conduct water through openings in their side walls. Knowing what type of wood species is being used will increase the understanding of the anatomical structure by revealing the locations of relative hardness and softness as well as the permeability of wood. The hardness refers to the sturdiness of the cell walls, which reflects to the amount of lignin and cellulose. For this research southern yellow pine wood is used to represent the guardrail posts. It is common for wood guardrail posts to be made of southern yellow pine.

To this point, the discussion has been over the structure and the properties of wood. It is very important to understand the wood characteristics in order to represent the engineering performance of a guardrail wood post. The objective of this research is to develop different material models of wood to predict the dynamic behavior of guardrail posts by doing a qualitative study.

2. PROCEDURES

A series of pendulum tests were performed by Texas A&M Transportation Institute (TTI) to dynamically determine the wood post performance when impacted by a pendulum. The main objective of this research is to find a wood material model that accurately matches the experimental data obtained from these tests. First the type, size, condition, description of the system, details of any apparatus, the methods employed and methods of analyzing the data for the series of pendulum tests that were performed is to be known and understood. The next step is to model the pendulum and the different guardrail posts needed to create the simulations. Then, three different material models are created for the simulation and analyzed to find which one of the material models match the best with the pendulum tests results.

As mentioned before, LS-DYNA program was utilized to perform the finite elements simulations. The Livermore Software Technology Corporation (LSTC) creates LS-DYNA and many other useful engineering software products through a team of engineers, mathematicians, and computer scientists [8]. LS-PrePost is an advance pre and post-processor designed for LS-DYNA. LS-PrePost's main post-processing capabilities include result animation, fringe component plotting, and XY history plotting. For this research, LS-PrePost is used to create the different material models and simulate the impact of a pendulum to the guardrail post. The three different material models are, 123 – Modified Piecewise Linear Plasticity, 143 – Wood, and 143 – Wood Pine.

Wood materials are much more challenging to characterize when modeling in LS-PrePost. LS-DYNA does not have a material model that is directly applicable to modeling the behavior of wood. The manual for LS-DYNA, Wood material Model 143 provides a description of the wood material for Southern Yellow Pine. This manual helps understand the theory and parameters that

are used as a reference to obtain an accurate simulation of a wood material post. For modeling purposes, the distinction between the tangential and radial directions is not always significant. Therefore, this manual uses the term perpendicular to the grain when no distinction is made between the radial and tangential directions, and parallel to the grain to describe the longitudinal direction [9].

2.1. Pendulum Tests

Physical testing of components is an important aspect of any design process. Four physical guardrail posts were tested at the TTI Proving Ground outdoor pendulum testing facility on September 30, 2016. This test includes a pendulum equipped with a rigid nose with two pipe cylinders attached to the nose and various CRT and standard posts. A CRT post has a drilled hole approximately 44 inches deep, just above the ground line and on the contrary a standard post is a solid wood post with no holes. All posts measured 6 feet in length and were installed 40 inches into the post box and 32 inches above the ground line. Each test was done to dynamically determine the post's performance when impacted by a pendulum bogie at a nominal target speed of 10 mph and at a height of 18 inches above the ground, to represent the bumper height of a small passenger car. The pendulum test and data analysis procedures were in accordance with guidelines presented in *NCHRP Report 350* [16].

Timber guardrail posts are roadside safety devices used to support W-beam guardrail in soils. These posts and guardrail systems serve to capture and redirect a vehicle during an impact. The four guardrail posts tested included a CRT post in the 'weak' and 'strong' direction and a standard wood post in the 'weak' and 'strong' direction. Depending upon the test parameters, each test was designed to impact that post from either the roadway side in the 'strong' direction

of the post, or the upstream side in the ‘weak’ direction of the post. Wooden shims were installed as needed to secure each post to a snug fit in the post box.

Two accelerometers were mounted at the rear of the bogie to measure longitudinal acceleration levels. Electronic signals from the accelerometers were amplified and transmitted to a base station through a constant bandwidth FM/FM telemetry link for recording on magnetic tape and for display on a real-time strip chart. Calibration signals were recorded before and after the test and an accurate time reference signal was simultaneously recorded with the data. Pressure sensitive switches on the nose of the bogie were actuated by wooden dowel rods and initial contact to produce speed trap and "event" marks on the data record to establish the exact instant of contact with the installation, as well as impact velocity.

The data is then received, recorded and digitized. A program was then used to convert the analog data from each transducer into engineering units. The data that was converted was then used with the Test Risk Assessment Program (TRAP) which uses the data to compute occupant/compartment impact velocities, time of occupant/compartment impact after bogie impact, and the highest 10-ms average ridedown acceleration. For reporting purposes, the data from the bogie-mounted accelerometers were then filtered with a 180 Hz digital filter and plotted using a commercially available software package.

2.2. Finite Elements Simulation of Posts and Pendulum

Details from the physical test were used to design the model of the pendulum on LS-PrePost. Figure 4 shows the model of the pendulum that was developed to use for the simulation. The pendulum was equipped with a rigid nose with two pipe cylinders attached to the nose. The mass for the pendulum was set to be 0.880 tons, 1945 lbs. Each part of the pendulum was established to simulate the material that was used for the physical pendulum test.

Figure 5 shows the model of the four different posts used for the simulations. The posts evaluated in this study were of a southern yellow pine CRT post and a standard wood post. The CRT wood post has a hole drilled in the post, which is meant to allow the post breakaway upon impact. Depending on the simulation parameters, each test simulation was designed to impact the post at a specific orientation, to represent the "strong" direction and "weak" direction.

From left to right, the first post represents a CRT posts in the strong direction, the second post is a CRT in the weak direction. The third post represents a standard timber post in the strong direction and the last post is a standard timber post in the weak direction. Wood measurements for all posts were set to 6" x 8" x 6'. A sleeve was modeled to hold the post and a shim to fill the gap between the post and sleeve to secure each post to fit in the post box. The pendulum is suspended by cable and was set to impact the guardrail posts at a nominal target speed of 10 mph and at a height of 18 inches above the ground.

2.3. Material Models

Three different material models were selected to create the characteristics of the wood material. These three material models are Material Model 123 Modified Piecewise Linear Plasticity, Material Model 143 Wood, and Material Model 143 Wood Pine. Each of the material models requires different inputs to represent the material model. The values used for the materials are based on the evaluation of the model through correlations with wood post data given by Murray and Reid and clear wood data for southern yellow pine, as default available properties given by Green and Kretschmann. For this study, the density for all material models was set to 6.63E-10 tons/mm^3. It was based on the density calculated on an actual wood guardrail post used for testing. This density was also compared to an average density of a southern yellow pine wood, being a 2% error from the original value.

2.3.1. Material Model 123 Modified Piecewise Linear Plasticity

The material type 123 is an elasto-plastic material supporting an arbitrary stress versus strain curve as well as arbitrary strain rate dependency. This material model has six important parameters to create the characteristics of southern yellow pine. Table 1 shows these six parameters used for the material model.

The first parameter is density, as stated before this value is set to 6.63E-10 ton/mm^3. For Southern Yellow Pine wood the Young Modulus ranged from 11750 MPa to 16720 MPa, the range was based on moisture content. A Young Modulus of 11750 MPa was selected for both the CRT and standard post. Poisson's ratio for southern yellow pine is approximately 0.3. The yield stress ranged from 40 to 60 MPa. In this study the value of 60 MPa was selected for both the CRT and standard post. Tangent modulus was selected to be 88 MPa according to the literature [2, 8, 10, 11]. The major in plane strain at failure were input values that varied depending if the wood posts was a CRT or a standard wood post based on its orientation. This value is used to determine the failure.

2.3.2. Material Model 143 Wood

Material Model 143 wood is a transversely isotropic material in which the properties in the tangential and radial directions are modeled the same. For simplicity, the longitudinal direction is referred to as the parallel to the grain direction and the tangential and radial directions as the perpendicular to the grain direction. This material model has the option on the user to input his or her own material properties. Table 2, Table 3, Table 4 and Table 5 show the parameters used for each wood post in the simulation. The four tables below are based on the moisture content and the quality factor in tension and compression.

Depending on the moisture content, all the inputs for the target material are changed. Four different moisture contents, 1%, 7%, 12%, and 23%, were selected to understand the difference between them and how it affected the failure of the wood posts. The inputs used for all wood posts are found in appendix B. As a result, as the moisture content decreases the material becomes stronger. In a fully saturated wood, 23%, the wood is weaker than for a less saturated wood. A moisture content of 12% was then selected for all wood post, since the data resembled the best to the pendulum tests. Also it is typical for moisture content of wood post testing to be around an average of 12%.

The elastic properties were based on averages provided by the Wood Material Manual 143 for southern yellow pine. It should be noted that these averages are based on clear wood, meaning no defects are found in the wood. The elastic properties inputs depended on the moisture content that was chosen. E_L is the normal modulus of the undamaged wood parallel to the grain, the L referring to the longitudinal direction. E_T refers to the normal modulus of the undamaged wood perpendicular to the grain, the T referring to the tangential direction, and since it is a transversely isotropic model, it also the same as R, radial direction. G_{LT} and G_{LR} are the shear modulus of the undamaged wood parallel and perpendicular to the grain, respectively. V_{LT} is Poisson's ratio parallel to the grain. A transversely isotropic material has three ratios, but only one of which is independent.

The clear wood strength parameters were also based on average data for southern yellow pine. X_T, X_C and $S_{\parallel}$ are the strengths parallel to the grain. They are in uniaxial tensile stress, uniaxial compressive stress, and pure shear stress, respectively. Together these three strengths form an irregular elliptical surface for modeling failure or yielding parallel to the grain and form the ultimate yield surface. Y_T, Y_C and $S_{\perp}$ are the strength perpendicular to the grain. They are in

uniaxial tensile stress, uniaxial compressive stress, and pure shear stress, respectively. The yield surface for the perpendicular modes is separate from the yield surface for the parallel modes.

However, these values depended on the moisture content and the tension and compression strength reduction factors. Because the strength of graded wood posts is less than that of clear wood posts, the clear wood strength must be scaled down according to the grade. These two scale factors are the tension/shear quality factor (Q_t) and compression quality factor (Q_c). Q_t reduces the tensile and shear strengths as a function of grade and Q_c reduces the compressive strengths as a function of grade. The grade of wood includes an assessment of wood defects. When analyzing the structure of guardrail posts, the exact position of the defects is not known. Therefore, a practical approach for addressing the defects is to modify the material properties globally as a function of visual grade [5]. This approach requires the implementation of the grade as an input parameter. For this study, the wood post grade was selected for a 1, 1D, 2, and 2D visual grade. The default values for Q_t and Q_c reduction factors are 0.47 and 0.63 for southern yellow pine wood. The values for strength were calculated by multiplying the quality factor for tension and compression depending if that parameter was in tension or compression.

The damage model requires an input of eight damage parameters, four for the parallel modes and four for the perpendicular modes. $Dmax_{\parallel}$ is the damage that can accumulate parallel to the grain. The damage accumulation is based on an undamaged elastic strain energy norm formulated from the parallel strains. $Dmax_{\perp}$ is the maximum damage that accumulates perpendicular to the grain. The damage accumulation is based on an undamaged elastic strain energy norm formulated from the perpendicular strains. The typical values for the maximum damage parameters are $dmax_{\parallel} = 0.9999$ and $dmax_{\perp} = 0.99$. The values are slightly less than one to avoid potential computational difficulties associated with zero stiffness for dmax = 1. The

parallel damage parameter is closer to 1 than the perpendicular parameter because elements erode with maximum parallel damage, but not with maximum perpendicular damage [5]. For parameters D and B, the default values were set to 30. The two parameters set the shape of the softening curves plotted as stress-strain or stress-displacement. Since there is no data available to set the shape of the softening curves so they have been arbitrarily chosen. The fracture energies are based on the FPL reported data for southern yellow pine, clear wood [15]. Default fracture energies for the perpendicular modes are selected depending on the moisture content. These values are default regardless of the temperature or grade of the wood. To accommodate variation with grade, the parallel to the grain fracture energies are found using the following equations.

$$G_{fI||} = 106 G_{fIper} Q_T \qquad G_{fII||} = 106 G_{fIIper} Q_T \tag{3}$$

Where G_{fIper} and G_{fIIper} are clear wood fracture energy values for southern yellow pine and as mentioned before Q_t and Q_c are scale factors. These equations indicate that the default fracture energies for clear wood, parallel to the grain, is 106 times greater than the default fracture energy perpendicular to the grain [5].

The last parameters needed in this material model are the hardening parameters $N||$, $c||$, $N_\perp$ and $c_\perp$. $N||$ and $c||$ are for modeling prepeak nonlinearity in compression parallel to the grain while $N_\perp$ and $c_\perp$ are for modeling compression perpendicular to the grain. The values for hardening initiation in parallel and perpendicular, $N||$ and $N_\perp$, were set to 0.5 and 0.4, respectively. These values are independent of grade, temperature, and moisture content. Values for $c_{||}$ and $c_\perp$ depend on the wood grade, but are independent of temperature and moisture content. These hardening parameters are obtained following equation 4:

$$c_{||} = \frac{400}{Q_c}\ Parallel \qquad c_{||} = \frac{100}{Q_c}\ Perpendicular \tag{4}$$

2.3.3. Material Model 143 wood pine

Material Model 143 wood pine is also a transversely isotropic material that uses default material properties for southern yellow pine wood. Table 6 shows the different parameters used for this model. The density was set to 6.63 ton/mm^3.

The input hard is an additional hardening parameter. This parameter allows each translating yield surface to surpass the ultimate yield surface. A positive value will produce continued hardening in excess of the yield strengths and a zero value will produce perfect plasticity in compression [5]. A small positive value is recommended if computational difficulties are suspected because of perfect plasticity. In this case 0.05 was selected as the input value. Moisture content for this material model was set to 12%. The temperature was left at the default value, 20°C.The parameters Q_t and Q_c, are the only parameters that varied depending on the type of post and the orientation. Qt and Qc are the implementation of addressing global strength reduction factors as a function of grade. In this model AOPT is available to create the wood direction. The A are the coordinates, that are parallel to the grain direction and D are components that are perpendicular to the grain directions.

3. RESULTS

Figuring out the most accurate material model for a wood guardrail post required a variety of simulations which were developed to acquire the most accurate material model. Three different material models were developed and compared to results from the field tests. For the field tests a total of eight pendulum tests were conducted, for the simulations a total of twelve were developed. For the simulation, there was an error found since the pendulum caused some vibrations after impact leaving some undesirable data. While these issues may affect the data, it was believed that the data was not greatly influenced by them and as a result the data after impact was not used. Both the pendulum test and simulation results were compared by only using data until there was no contact between the pendulum and guardrail post. The data was processed for each simulation to obtain the longitudinal acceleration curves. This section discusses the results for the CRT and standard wood post in the strong and weak axis based on the three different material models. The simulation results were compared to experimental acceleration data.

3.1. Controlled Release Terminal Post – Strong Axis

Three CRT wood posts in the strong axis were tested by TTI. Figure 6 shows the longitudinal acceleration results from these three tests. Two of the pendulum tests had very similar responses whereas the other test showed somewhat a stronger response. A variation of the responses can be because of the many factors affecting wood, such as the moisture content or defects found in the wood. Test P4 fractured completely through the post after impact at 0.019 seconds and lost contact at 0.035 seconds. For test P5, it fractured at 0.012 seconds and lost contact with post at 0.033 seconds. For the last test in this case, P8, the post fractured completely at 0.010 seconds and at 0.05 seconds the pendulum lost contact with the post.

3.1.1. Material Model 123 Modified Piecewise Linear Plasticity

The first simulation includes material model 123 modified piecewise linear plasticity for a CRT wood post in the strong axis. The parameters for this material model are found in Table 1. Figure 7 shows the sequential images of the simulation. The CRT wood post fractures as a result of the impact and lost contact with the pendulum at approximately 0.02 seconds.

Figure 8 shows the acceleration curves for the pendulum test and the simulation. The material model was sought to produce a response resembling the three similar pendulum tests. It can be observed that the simulation from this material model has some similarities to the pendulum tests. The peaks of acceleration are in the range, the break happens earlier than the pendulum tests. This can be because the post from the simulation was weak. In the simulation test, the guardrail post fractured completely at 0.01 seconds after impact.

3.1.2. Material Model 143 Wood

The following simulation uses material model 143 wood for a CRT wood post in the strong axis. The parameters used for this model are found in table 2. Figure 9 shows a series of images of the simulation. The CRT wood post fractures as a result of the impact and lost contact with the pendulum at approximately 0.025 seconds.

Figure 10 displays the acceleration curves for the pendulum test and the simulation. The material model was sought to produce a response resembling the three similar pendulum tests. It can be seen that by using this material model the response did not resemble the test results as expected. The reason for not resembling the pendulum test result could be because of the effect of each parameter value, when changing one parameter, it affects the results.

3.1.3. Material Model 143 Wood Pine

For the following simulation, material model 143 wood pine was used for a CRT wood post in the strong axis. Figure 11 shows the sequential images of the simulation from 0.0 seconds to 0.075 seconds. The CRT wood post fractures as a result of the impact and lost contact with the pendulum at approximately 0.02 seconds.

Figure 12 shows the acceleration curves for the pendulum tests and the simulation. The material model in this case resembled the pendulum tests. Initial acceleration peaks from the pendulum test ranged from -9 g to -16 g, and for the simulation peak it was approximately -7 g. The simulation shows an acceptable similarity and seems to be the most accurate material model when compared to the other material model simulations.

3.2. Controlled Release Terminal Post – Weak Axis

For the CRT post in the weak axis, two pendulum tests were conducted by TTI. Figure 13 displays the longitudinal acceleration of the two tests that were performed. The two pendulum tests had very similar responses. For test P6, the post fractured completely through at 0.012 seconds after impact, test P7 as well completely fractured at 0.012 seconds.

3.2.1. Material Model 123 Modified Piecewise Linear Plasticity

Material model 123 modified piecewise linear plasticity was used for a CRT wood post in the weak axis. The parameters for this material model are found in Table 1. Figure 14 presents the sequential images of the simulation. The CRT wood post lost contact with the pendulum at approximately 0.25 seconds.

Figure 15 shows the acceleration curves for the pendulum tests and the simulation. The material model was sought to produce a response resembling the two similar pendulum tests. It can be observed that the simulation response is almost similar to the pendulum tests; however it

seems to be stronger than the tests. The simulation response has similar initial peak acceleration that is in -7 to -10 g range, the peak for the simulation happens approximately 0.003 seconds before the physical tests.

3.2.2. Material Model 143 Wood

The following simulation uses material model 143 wood for a CRT wood post in the weak axis. The parameters used for this model are found in table 3. Figure 16 shows the sequential images for the simulation from 0.0 seconds to 0.07 seconds.

Figure 17 shows the acceleration curves for the two pendulum tests and the simulation. The material model was sought to produce a response resembling the two similar pendulum tests. It can be seen that by using this material model, the response did not resemble the test results.

3.2.3. Material Model 143 Wood Pine

For the following simulation, material model 143 wood pine was used for a CRT wood post in the weak axis. Figure 18 shows a series of images from the simulation. The CRT wood post fractures as a result of the impact and lost contact with the pendulum at approximately 0.03 seconds.

Figure 19 shows the acceleration curves for the pendulum test and the simulation. The simulation response has similar initial peak acceleration that is in -8 to -10 g range, although the peak for the simulation happens at approximately 0.004 seconds and the pendulum tests peak happens at 0.007 seconds.

3.3. Standard Timber Post – Strong Axis

For this case, only one pendulum test was conducted by TTI. As a result, the standard wood post in the strong axis did not fail immediately as the other wood posts. The post had a higher

strength than the other wood post cases. The following simulation results were compared to the pendulum test results shown in Figure 20. At 0.32 seconds after impact, the post fractured.

3.3.1. Material Model 123 Modified Piecewise Linear Plasticity

Material model 123 modified piecewise linear plasticity for a standard wood post in the strong axis was developed. The parameters for this material model are found in Table 1. Figure 21 displays the sequential images of the simulation.

Figure 22 shows the acceleration curves for the pendulum test and the simulation. In comparison, it can be observed that the simulation has similarities to the physical tests until approximately 0.035 seconds. After 0.035 seconds there is a difference showing that the results from the simulation represent a stronger wood post than the wood post from the pendulum test. The simulation results also show the wood post taking longer for it to fail.

3.3.2. Material Model 143 Wood

The following simulation uses material model 143 wood for a standard wood post in the weak axis. The parameters used for this model are found in table 4. Figure 23 shows a series of images from the simulation. The CRT wood post fails as a result of the impact and lost contact with the pendulum at approximately 0.03 seconds.

Figure 24 shows the acceleration curves for the pendulum test and the simulation. It can be seen that by using this material model that the response did not resemble the test results, concluding that it was not an accurate material model to use.

3.3.3. Material Model 143 Wood Pine

Material model 143 Woodpine was used for a standard wood post in the strong axis. Figure 25 shows the sequential images of the simulation at 0.0 seconds to 0.105 seconds. The CRT

wood post fractures as a result of the impact and lost contact with the pendulum at approximately 0.07 seconds. The fracture cannot be seen in the images but is represented in Figure 26.

Figure 26 shows the acceleration curves for the pendulum test and the simulation. The simulation shows some resemblance to the pendulum test. The only difference shown is the strength of the wood post. The simulation has a higher strength than the pendulum test.

3.4. Standard Timber Post – Weak Axis

Two pendulum tests were conducted by TTI for this case. Figure 27 shows the longitudinal acceleration results for the pendulum tests. The two pendulum tests had very similar responses. At 0.14 seconds after impact the post fractured for test P2 and for test P3 the post fractured at 0.010 seconds.

3.4.1. Material Model 123 Modified Piecewise Linear Plasticity

The following simulation includes material model 123 modified piecewise linear plasticity for a standard wood post in the weak axis. The parameters for this material model are found in Table 1. Figure 28 displays the sequential images of the simulation. The CRT wood post fractures as a result of the impact and lost contact with the pendulum at approximately 0.025 seconds.

Figure 29 shows the longitudinal acceleration curves for the pendulum tests and the simulation. The material model was sought to produce a response resembling the pendulum tests. It can be observed that the simulation response is also similar to the pendulum test responses. The simulation response has similar initial peak acceleration that is in -11 to -22 g range, the peak for the simulation happens approximately at 0.012seconds.

3.4.2. Material Model 143 Wood

The following simulation uses material model 143 wood for a standard wood post in the weak axis. The parameters used for this model are found in table 5. Figure 30 shows the sequential images of the simulation from 0.0 seconds to 0.07 seconds. The CRT wood post fractures as a result of the impact and lost contact with the pendulum at approximately 0.025 seconds.

Figure 31 shows the acceleration curves for the pendulum tests and the simulation. It can be seen that by using this material model that the response did not resemble the test results, concluding that it was not an accurate material model to use.

3.4.3. Material Model 143 Wood Pine

For the following simulation, material model 143 Woodpine was used for a standard wood post in the strong axis. Figure 32 shows the sequential images of the simulation. The CRT wood post fractures as a result of the impact and lost contact with the pendulum at approximately 0.02 seconds.

Figure 33 shows the acceleration curves for the pendulum tests and the simulation. The simulation shows resemblance to the pendulum test. The simulation response has similar initial peak acceleration that is in -11 to -22 g range, the peak for the simulation happens approximately at 0.012seconds.

4. DISCUSSION

Due to the wide variations of posts, many studies have been previously performed. Researchers have tested CRT post in different axes by performing several tests of a bogie impacting a post. Some of these tests were developed to determine the dynamic properties of the CRT wood posts to later assist in the design of steel posts by reproducing the existing properties of the CRT post observed in the dynamic bogie tests [10]. However, this study included the data of the pendulum tests performed by TTI which comprised of a CRT post and a standard post being impacted by a pendulum at different axes. The results gathered from the tests were of the variations for the longitudinal acceleration. This variation was caused by the influence of many factors that affect the strength of wood as well as the testing parameters.

Not every wood post behaves the same in failure but as shown in each of the pendulum tests, they had similar response based on the post and direction. This is displayed in figure 6, 13, 20, and 27. The strongest wood post was the standard post in the “strong axis”. One of the main reasons for such strength was because there was no large defect like the CRT post which had a hole close to the ground. The direction as well contributed with the strength of the post. On the contrary, the weakest post was the CRT in the weak axis because of the defect found on the wood post, the hole closed to the ground making it the failing region around the breakaway hole.

Finite element models of a CRT post have been developed and compared with pendulum tests data. Researchers have developed material models for the post as an isotropic elastic plastic model in which it sufficiently simulated the failure mode observed in wooden guardrail posts during impact. Their results were validated by performing a statistical analysis and concluded that the finite element model is realistic and can be used with confidence in an extensive model of a guardrail system [2]. This study involves three different material models used for each case.

Each material model has different parameters affecting the way the wood posts failure mode responds. It is not an easy task to create a material model that accurately simulates the breakaway characteristics of a wood post. There are challenges in selecting the appropriate parameters since moisture content and grade of wood have a major influence in the wood post failure.

Every input is very important and can affect the failure results of the wood post behavior when being impacted by the pendulum. Familiarizing with the background of wood and having data of the mechanical properties helps in deducing the values for each parameter. These values are gathered by following the Manual for LS-DYNA Wood Material Model 143 [5] and analyzing previous test values provided for southern yellow pine wood. Many tests have been conducted for clear southern yellow pine woods were the Young Modulus, Poisson's ratio, Shear Modulus and other properties are found [12,13]. Although it is important to understand that this value depends on many factors. A wood post varies in strength so when simulating the best that there can be to resemble a wood post is by getting as close as possible to the values for each parameter. This in turn gives an accurate response that can resemble within the pendulum tests of each case.

For each case, the best material model that accurately resembled the pendulum tests was material model 143 Woodpine. Many similarities can be observed from the comparison between the longitudinal acceleration plots. The events have an approximately same duration and the initial peak accelerations are within the ranges of each case. Material model 123 did resemble some of the tests but was not as accurate as material model 143 Woodpine. As for material 143 wood, it was the least accurate out of the other material models.

5. CONCLUSION

Understanding the properties of wood and having sufficiently reliable material parameters made it possible to develop three different material models where a CRT post and a standard post on the weak and strong axis were evaluated. For each result, the impact response of each material model varied when compared to the pendulum tests. The accuracy of the material models was based on the resemblance of the longitudinal acceleration to the longitudinal acceleration of the pendulum tests. The following conclusions can be drawn:

- Wood is a variable material. The type of species, moisture content, defects in the wood and age are important factors that influence the response of wood.
- Almost all properties are influenced by the moisture content of wood because as moisture content decreases, wood increases in strength, and when moisture content increases, wood decreases in strength.
- Material model 143 Woodpine responded with more accuracy compared to material model 123 Modified Piecewise Linear Plasticity and material model 143 Wood.
- Defects found in wood can affect the performance of the wood post and be the one of the main reasons for a wood post to fail.
- A CRT wood post is weaker in strength than a standard wood post. In a CRT post there is a drilled hole at the bottom and when impacted by a pendulum it is the primary reason for the wood post to fail, but in a controlled and predictable manner.
- Another important fact is that the direction of the wood post is important because it can affect the strength when being impacted. Placing wood posts in the “weak axis”, either a standard or CRT, show the wood post breaking at an earlier time than the post in the “strong axis”.

REFERENCES

[1] Nguyen, M. Q., J. D. Elder, J. Bayandor, R. S. Thomson, and M. L. Scott. *A Review of Explicit Finite Element Software for Composite Impact Analysis*. Journal of Composite Materials, Vol. 39. February 2005.

[2] Plaxico, C., Patzner, G., & Ray, M. *Finite-Element Modeling of Guardrail Timber Posts and the Post-Soil Interaction*. Committee on Roadside Safety Features. Transportation Research Record. 1998.

[3] Hoadley, R. Bruce., et al. *Understanding Wood: A Craftsmans Guide to Wood Technology.* Taunton Press. 2000.

[4] Winandy J. E., Arntzen, Charles J., *Wood Properties*. Encyclopedia of Agricultural Science. Orlando, FL: Academic Press: 549-561. Vol. 4. October 1994. https://www.fpl.fs.fed.us/documnts/pdf1994/winan94a.pdf

[5] Murray, Y.D. *Manual for LS-DYNA Wood Material Model 143*. Report No. FHWA-HRT-04-097. Federal Highway Administration. August 2007.

[6] Record, S.J. *The Mechanical Properties of Wood: Including a Discussion of the Factors Affecting the Mechanical Properties, and Methods of Timber Testing*. J. Wiley. 1914.

[7] Lamb, F.M. *Splits and Cracks in Wood.*Virginia Tech. 1992.

[8] *LS-PrePost Online Documentation and Tutorial*. Livermore Software Technology Corporation. Livermore, CA, May 2004.

[9] Arens S., Faller R., Rohde J., and Polivka K. *Dynamic Impact Testing of CRT Wood Posts in a Rigid Sleeve.* MnDOT, MwRSF Research Report No. TRP-03-198-08. April 2008.

[10] *Wood Structural Design Data.* American Wood Council. American Fores & Paper Association. 1986. http://www.awc.org/pdf/codes-standards/publications/wsdd/AWC-WSDD1986-ViewOnly-0301.pdf

[11] Green, D.W., and Kretschmann, D.E. *Moisture Content and the Properties of Clear Southern Pine.* Research Paper FPL-RP-531, Forest Products Laboratory,U.S. Department of Agriculture. 1994.

[12] Buchar J., Rolc S., Lisy J., and Schwengmeier, J. *Model of the Wood Response to the High Velocity of Loading.* International Symposium of Ballistics. Interlaken, Switzerland. May 2001.

[13] Bushchow, K.H.J. *Encyclopedia of Materials: Science and Technology*. Elsevier. 2001.

[14] Otkur, A. M. *Impact Modeling and Failure Modes of Composite Plywood.* Texas Tech University, December 2010.

[15] Stanzl-Tschegg, S.E., D.M. Tan, and E.K. Tschegg, *Fracture Resistance to the Crack Propagation in Wood.* International Journal of Fracture, Vol. 75, 1996, pp. 347-356, figure 1, p. 349, figure 3, p. 350.

[16] Ross JR, H.E., Sicking, D.L., Zimmer, R.A. Michie, J.D. *NCHRP Report 350: Recommended Procedures for the Safety Perfomance Evaluation of Highway Features.* American Association of State Highway and Transportation Officials in Cooperation with the Federal Highway Administration. Transportation Research Board National Research Council. Washington, D.C. 1993.

APPENDIX A

FIGURES

Figure 1. Southern Yellow Pine Growth Rings (adapted from Bruce Hoadley)[3]

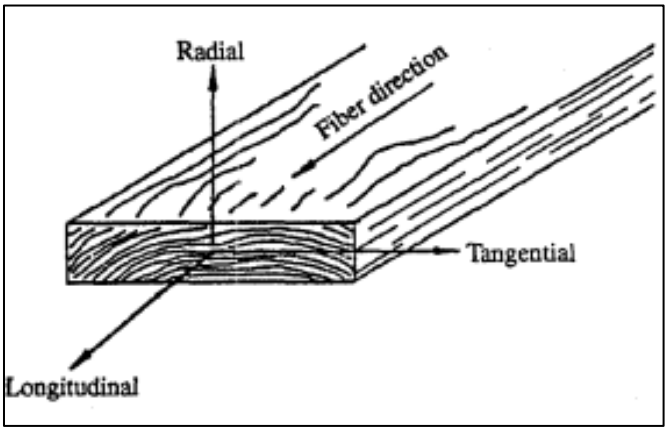

Figure 2. Three Principal Axes of Wood (adapted from Bushchow)[13]

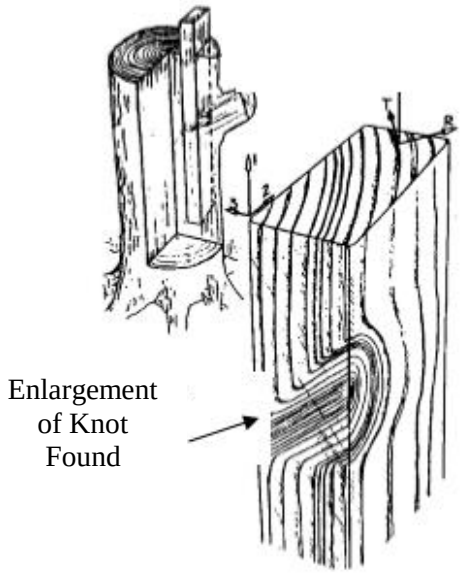

Figure 3. Knot Defect Found in a Board that has Been Cut Away From a Tree. (modified from Murray) [5]

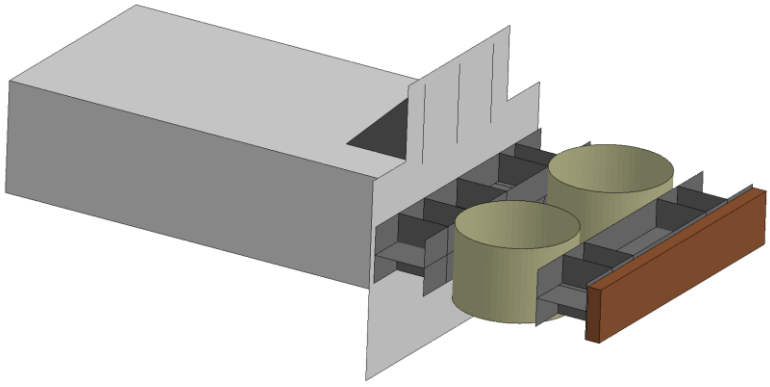

Figure 4. Pendulum Design Model

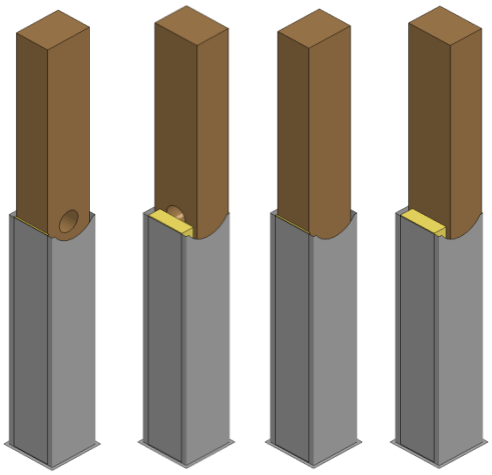

Figure 5. Wood Posts

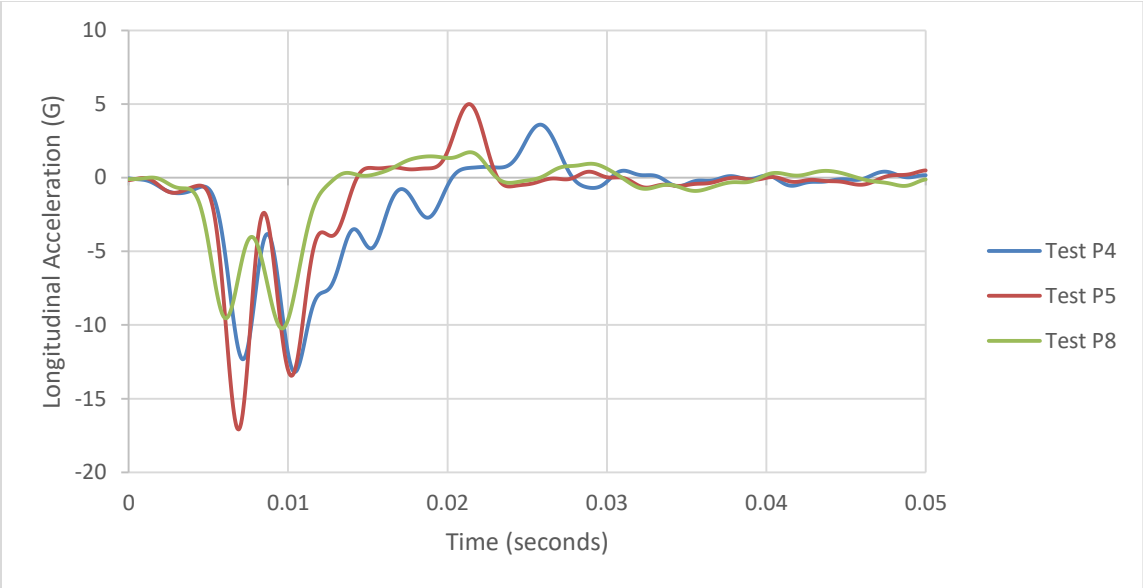

Figure 6. Longitudinal Acceleration for CRT Post in Strong Axis – Field Tests

Time = 0.0 seconds

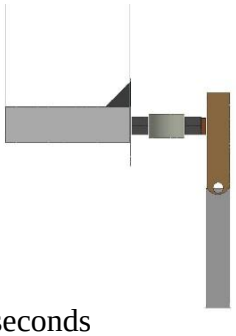

Time = 0.015 seconds

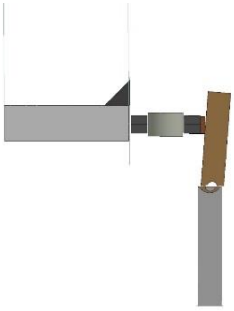

Time = 0.045 seconds

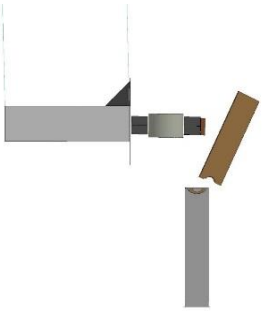

Time = 0.07 seconds

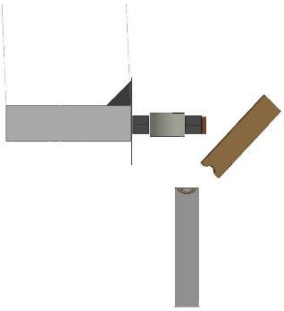

Figure 7. Sequential Images of CRT Post – Strong Axis (Material 123)

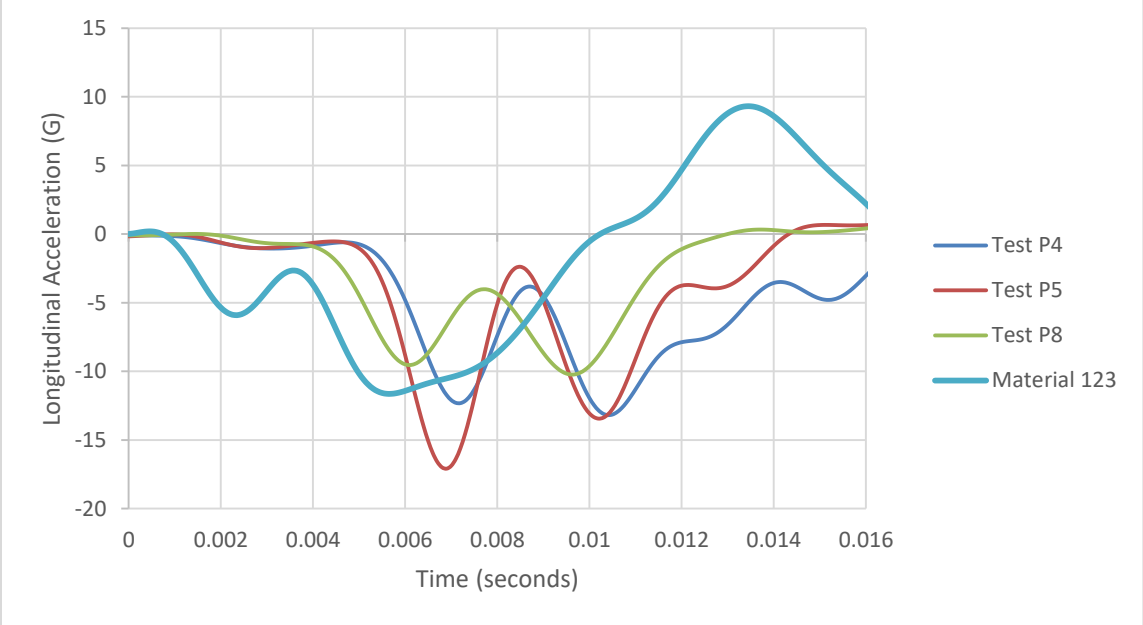

Figure 8. Longitudinal Acceleration for CRT Post in Strong Axis – Material 123

Time: 0.0 seconds

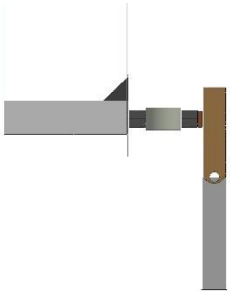

Time: 0.015 seconds

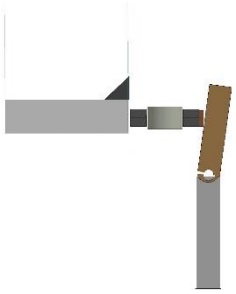

Time: 0.035 seconds

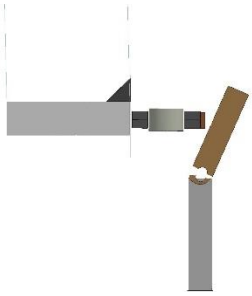

Time: 0.07 seconds

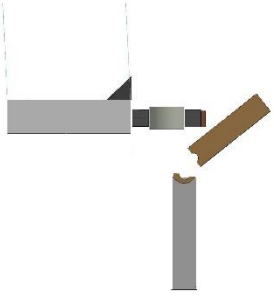

Figure 9. Sequential Images of CRT Post - Strong Axis (143 Wood)

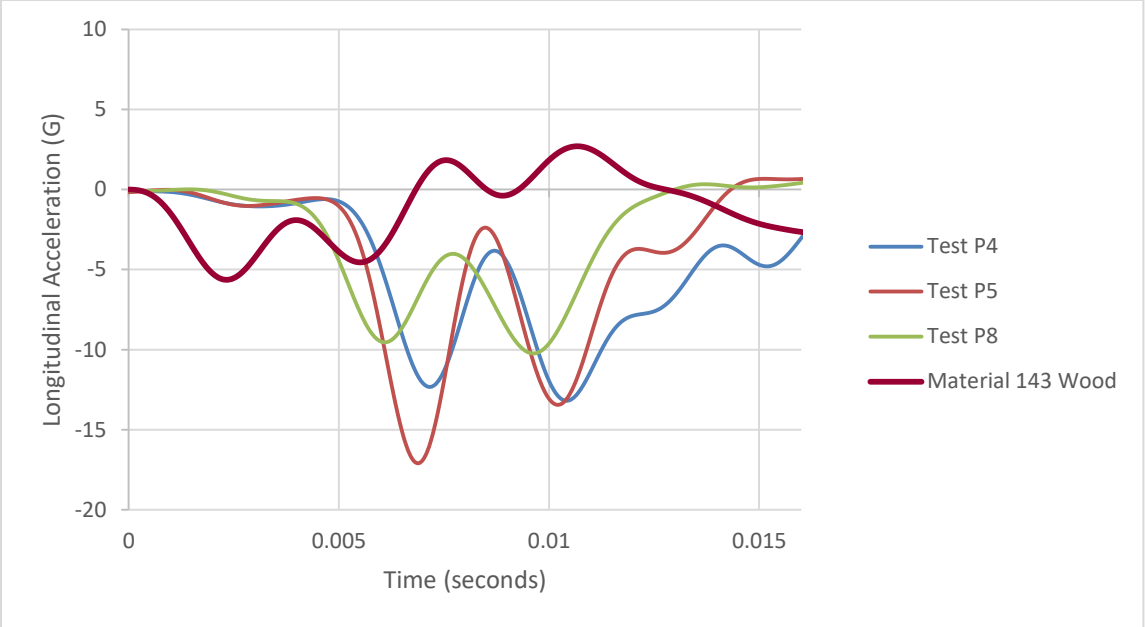

Figure 10. Longitudinal Acceleration for CRT Post in Strong Axis – Material 143 Wood

Time = 0.0 seconds

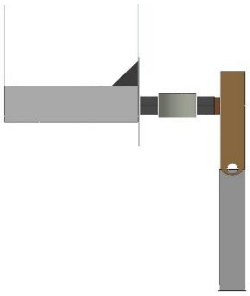

Time = 0.02 seconds

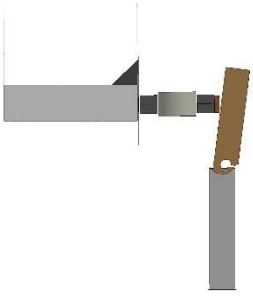

Time = 0.04 seconds

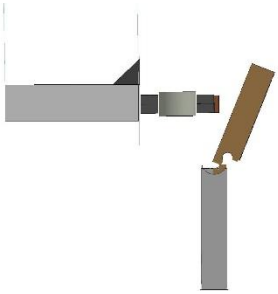

Time = 0.075 seconds

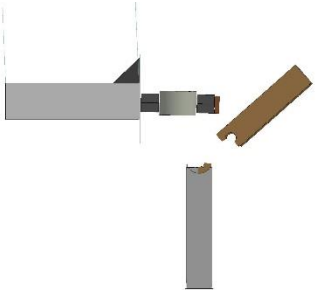

Figure 11. Sequential Images of CRT Post – Strong Axis (143 Wood Pine)

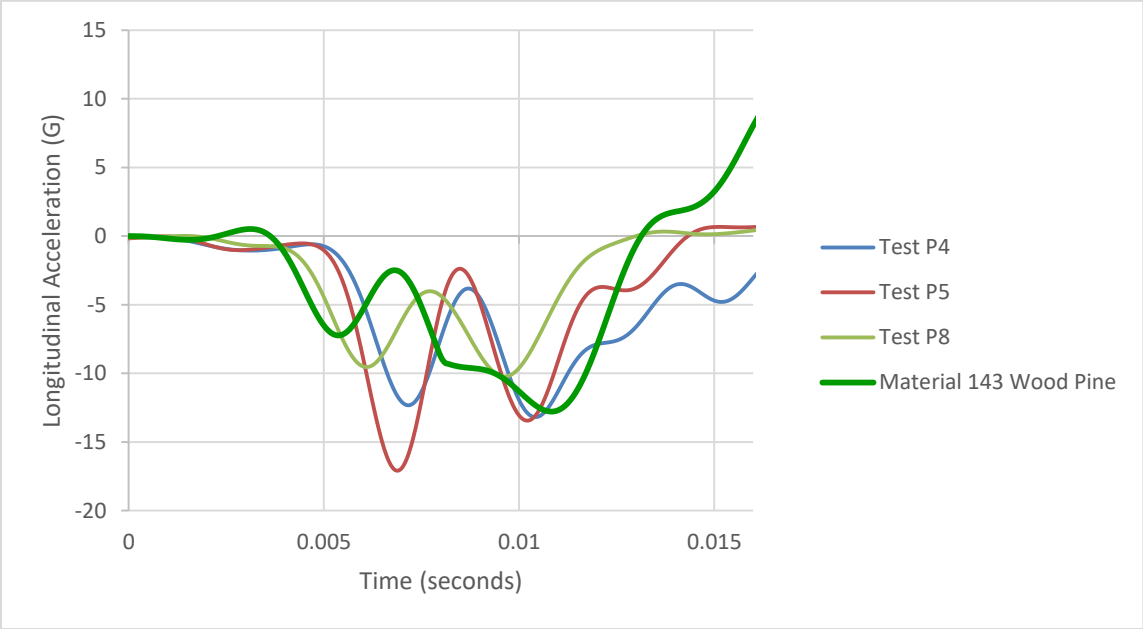

Figure 12. Longitudinal Acceleration for CRT Post in Strong Axis – Material 143 Wood Pine

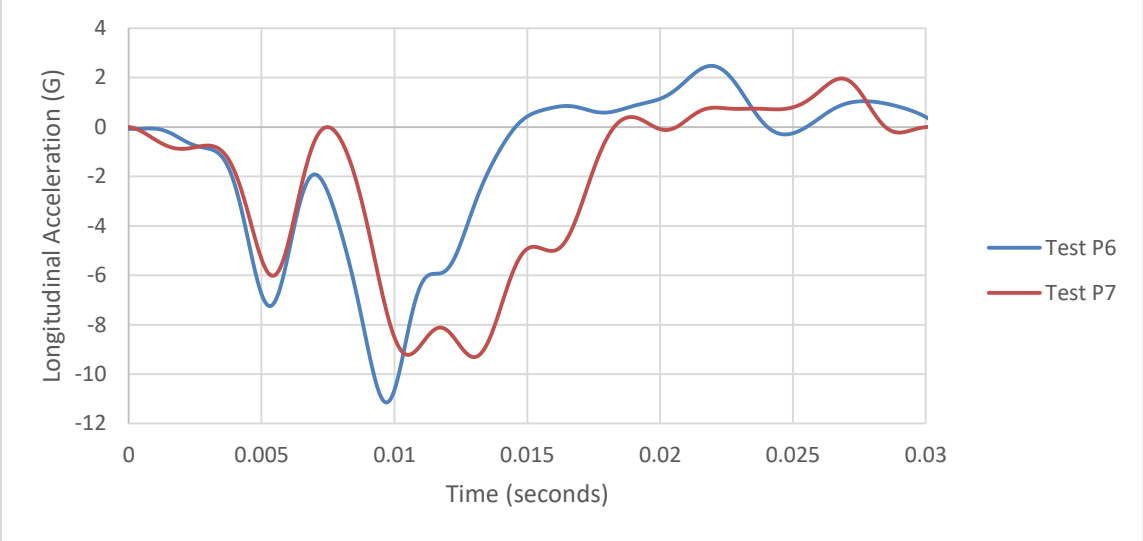

Figure 13. Longitudinal Acceleration for CRT Post in Weak Axis – Field Tests

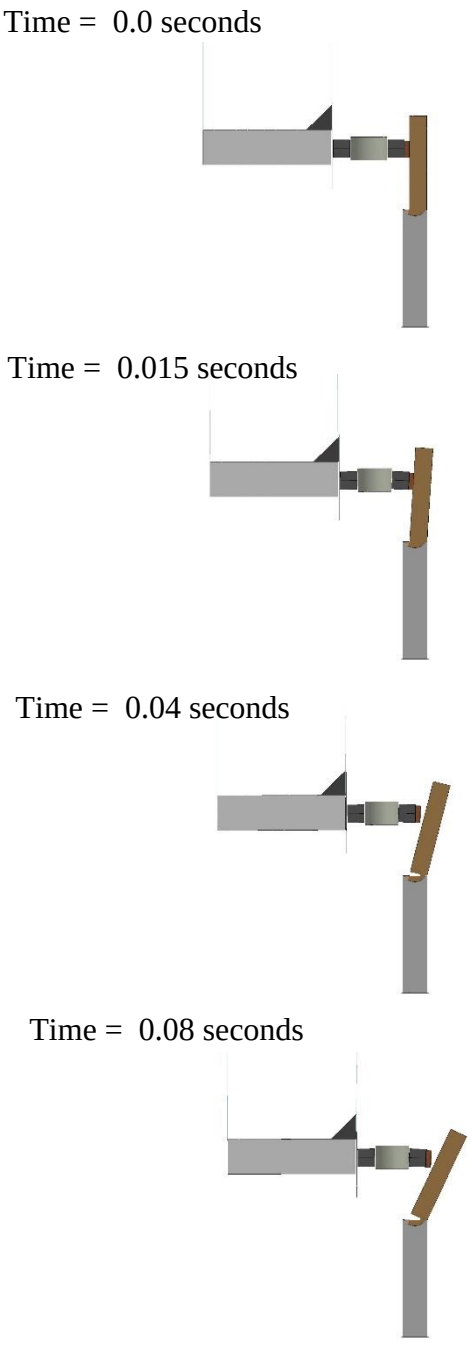

Figure 14. Sequential Images of CRT Post – Weak Axis (Material 123)

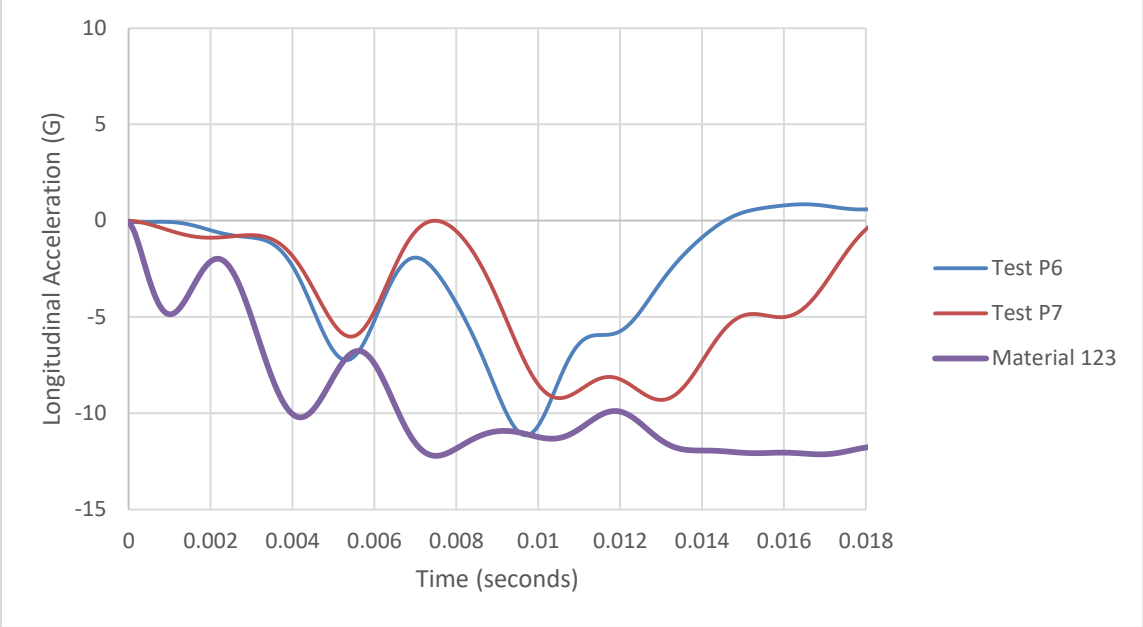

Figure 15. Longitudinal Acceleration for CRT Post in Weak Axis – Material 123

Time: 0.0 seconds

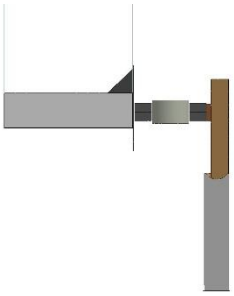

Time: 0.015 seconds

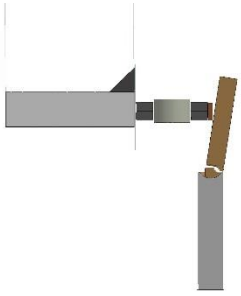

Time: 0.035 seconds

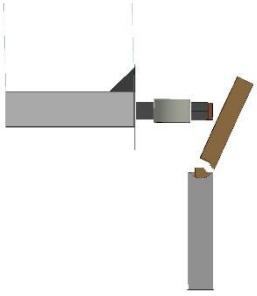

Time: 0.06 seconds

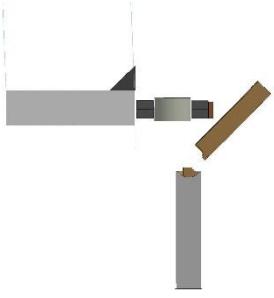

Figure 16. Sequential Images of CRT Post - Weak Axis (143 Wood)

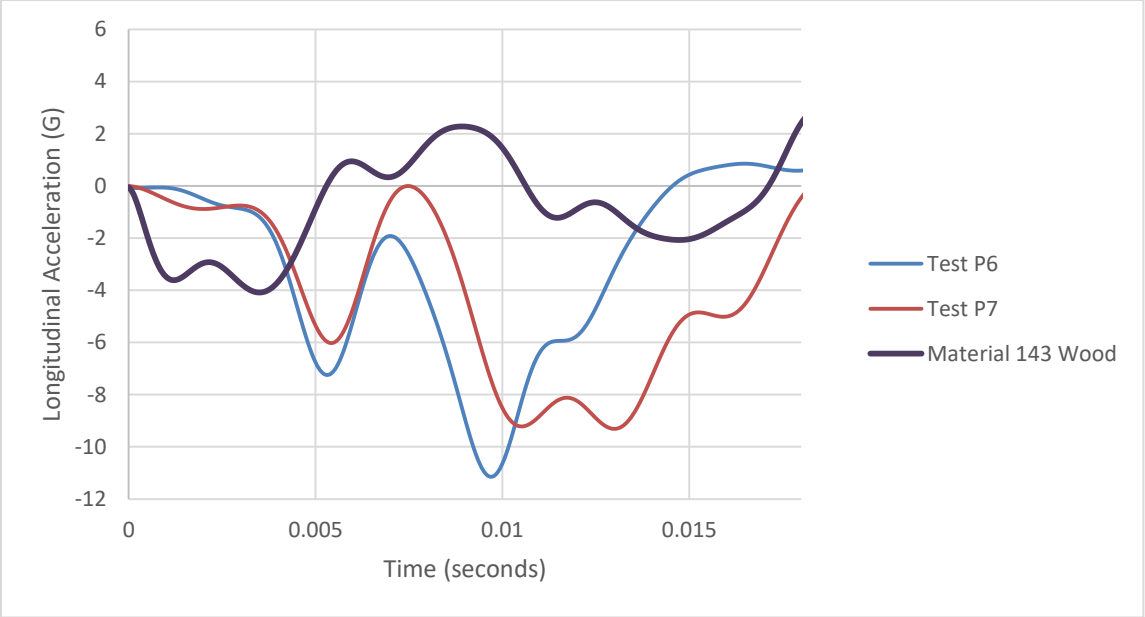

Figure 17. Longitudinal Acceleration for CRT Post in Weak Axis – Material 143 Wood

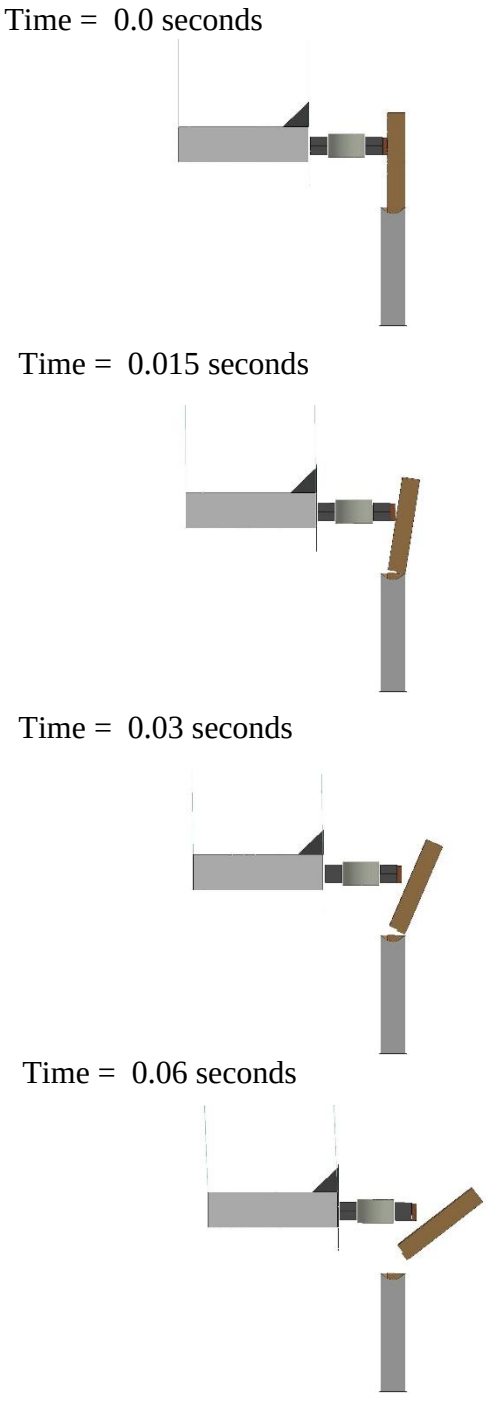

Figure 18. Sequential Images of CRT Post – Weak Axis (143 Wood Pine)

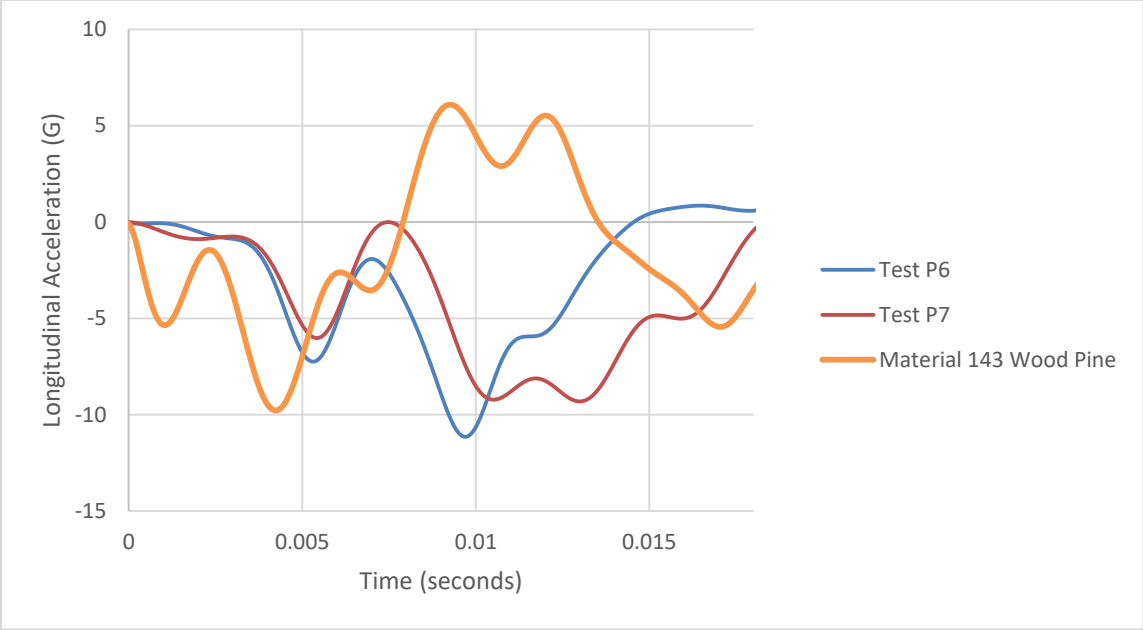

Figure 19. Longitudinal Acceleration for CRT Post in Weak Axis – Material 143 Wood Pine

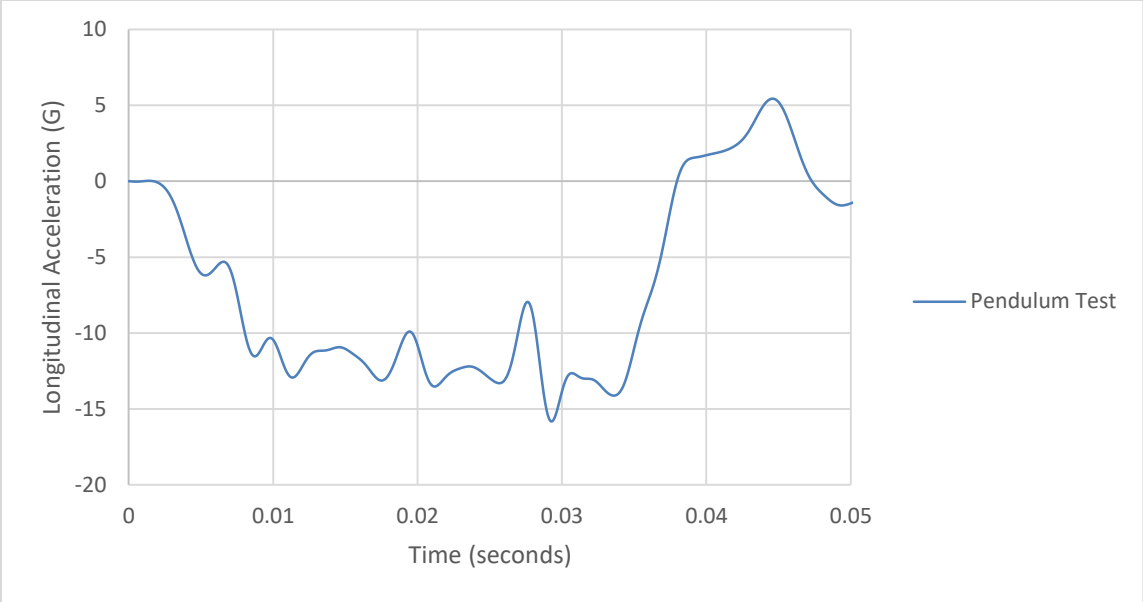

Figure 20. Longitudinal Acceleration for Standard Post in Strong Axis – Field Test

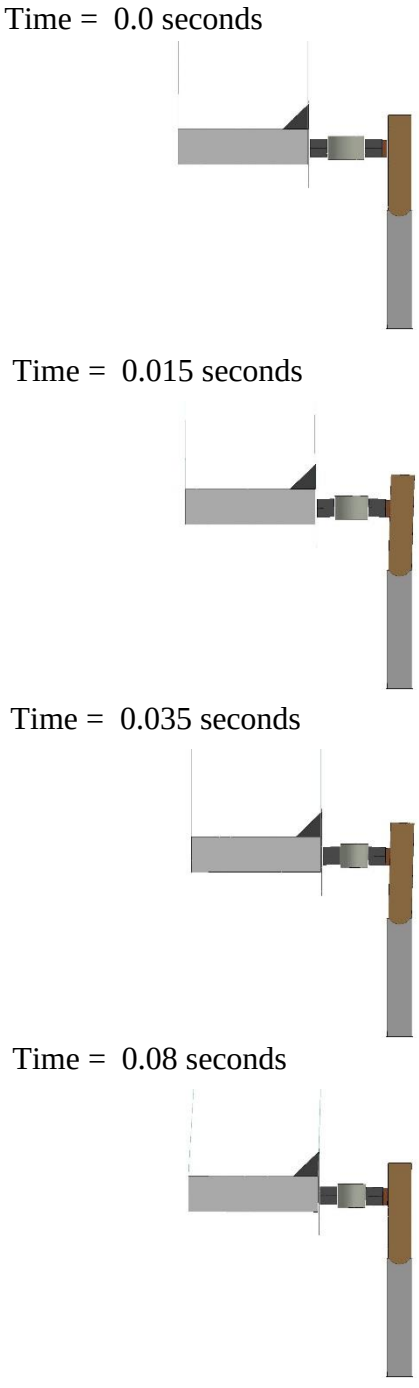

Figure 21. Sequential Images of Standard Post – Strong Axis (Material 123)

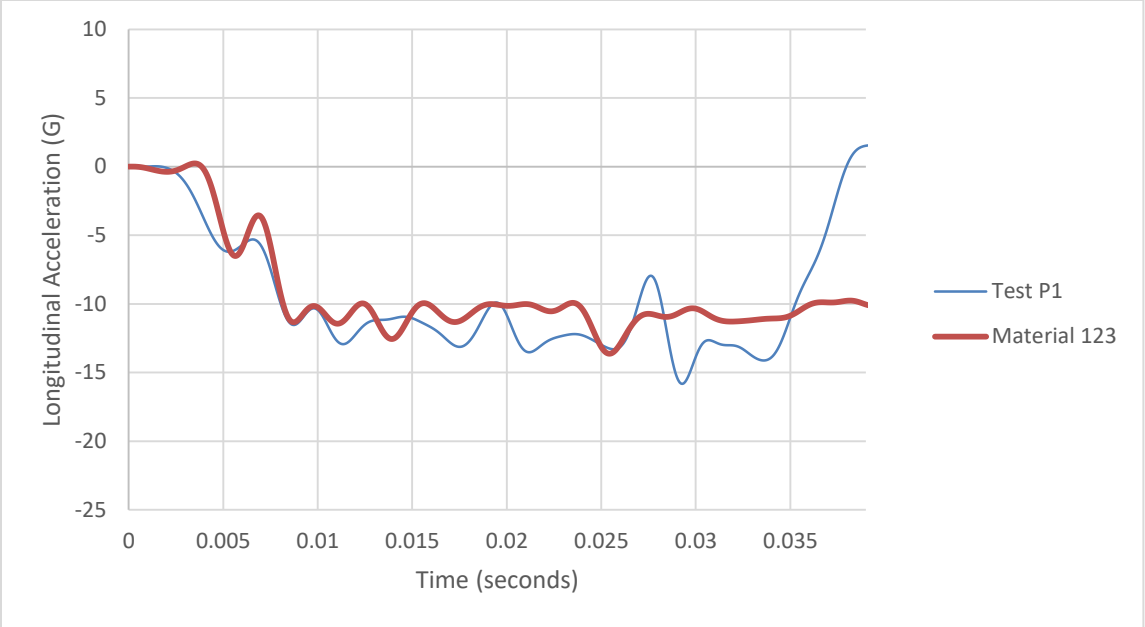

Figure 22. Longitudinal Acceleration for Standard Post in Strong Axis – Material 123

Time: 0.0 seconds

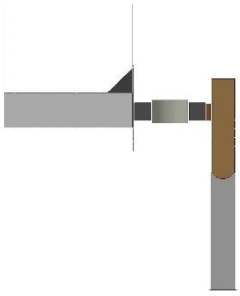

Time: 0.015 seconds

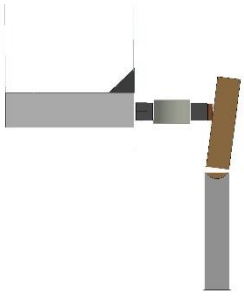

Time: 0.035 seconds

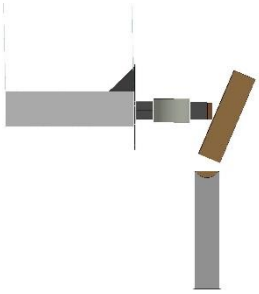

Time: 0.065 seconds

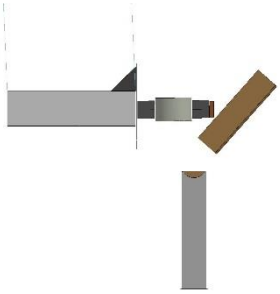

Figure 23. Sequential Images of Standard Post - Strong Axis (143 Wood)

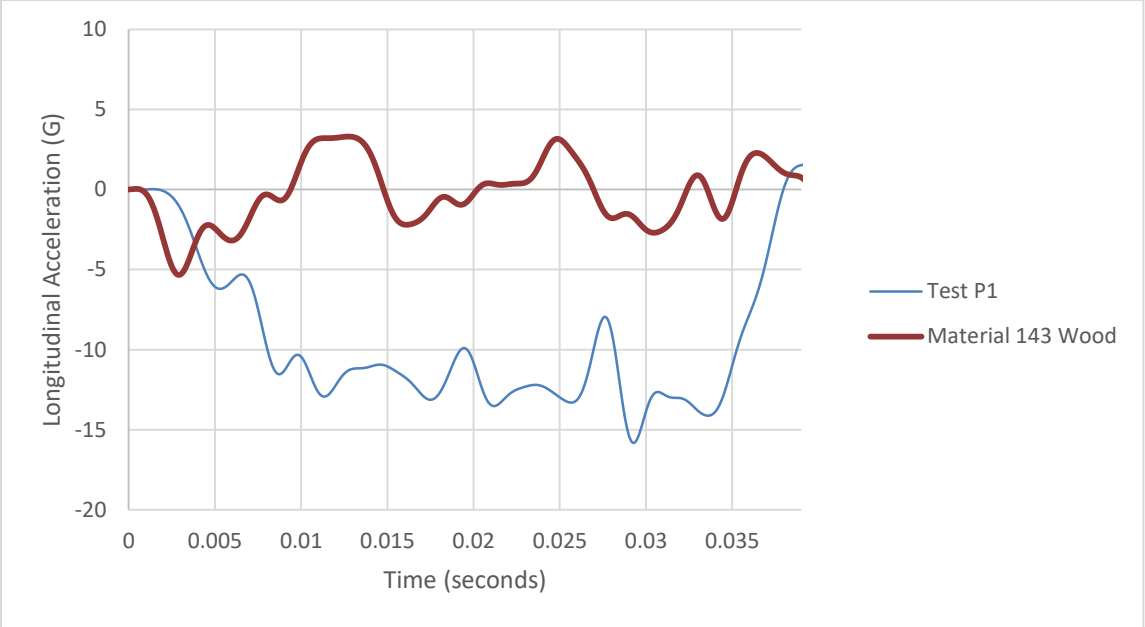

Figure 24. Longitudinal Acceleration for Standard Post in Strong Axis – Material 143 Wood

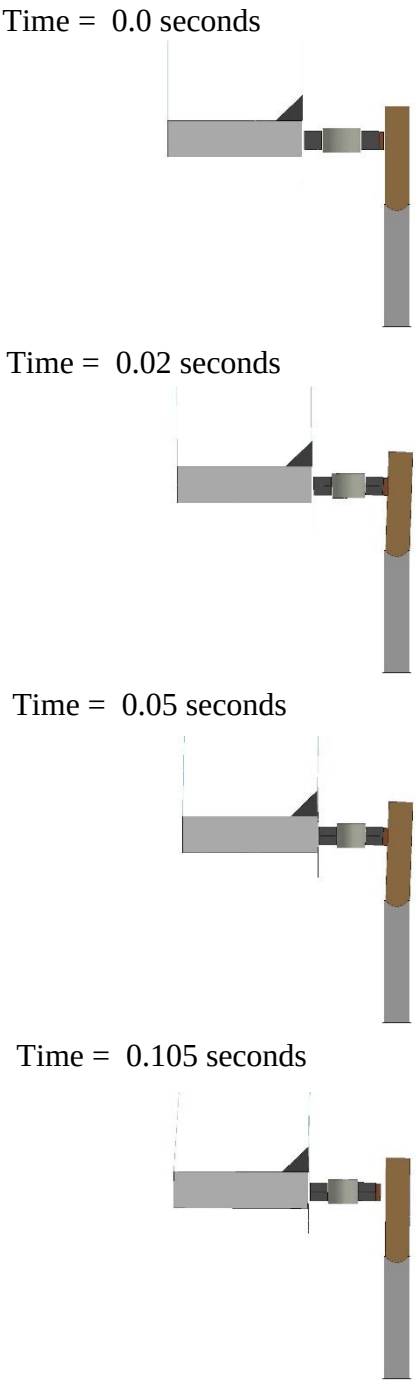

Figure 25. Sequential Images of Standard Post - Strong Axis (143 Wood Pine)

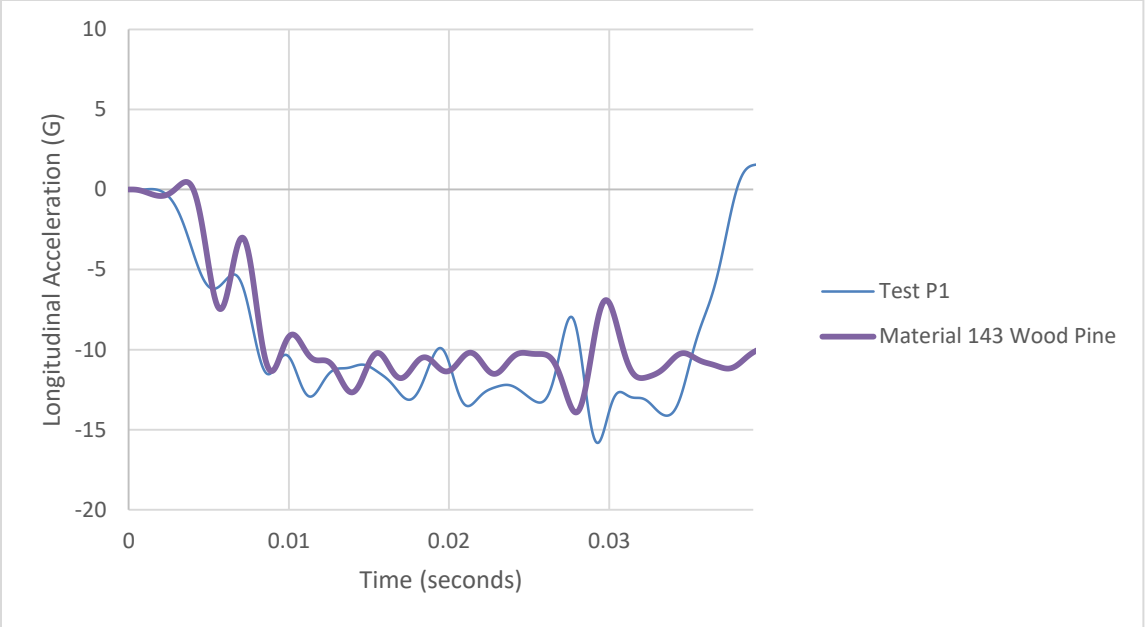

Figure 26. Longitudinal Acceleration for Standard Post in Strong Axis – Material 143 Wood Pine

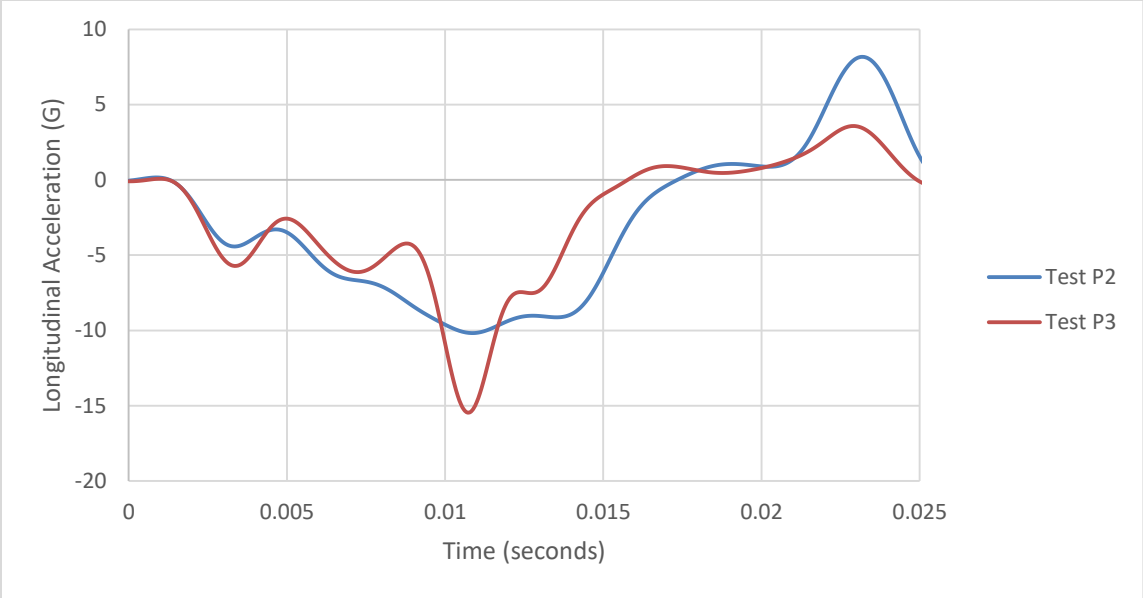

Figure 27. Longitudinal Acceleration for Standard Post in Weak Axis – Field Tests

Time = 0.0 seconds

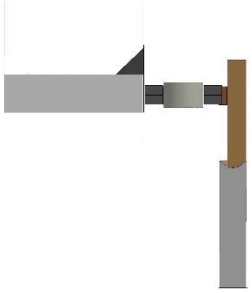

Time = 0.015 seconds

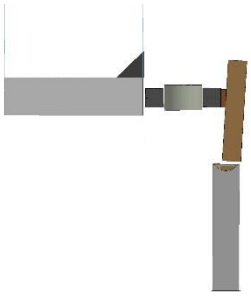

Time = 0.04 seconds

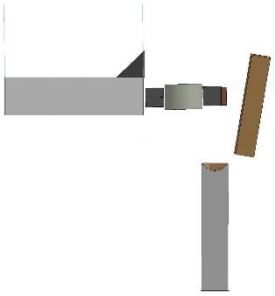

Time = 0.07 seconds

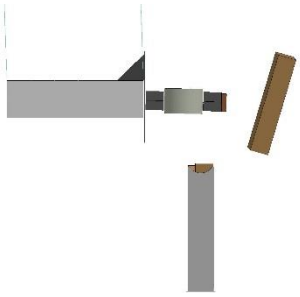

Figure 28. Sequential Images of Standard Post - Weak Axis (Material 123)

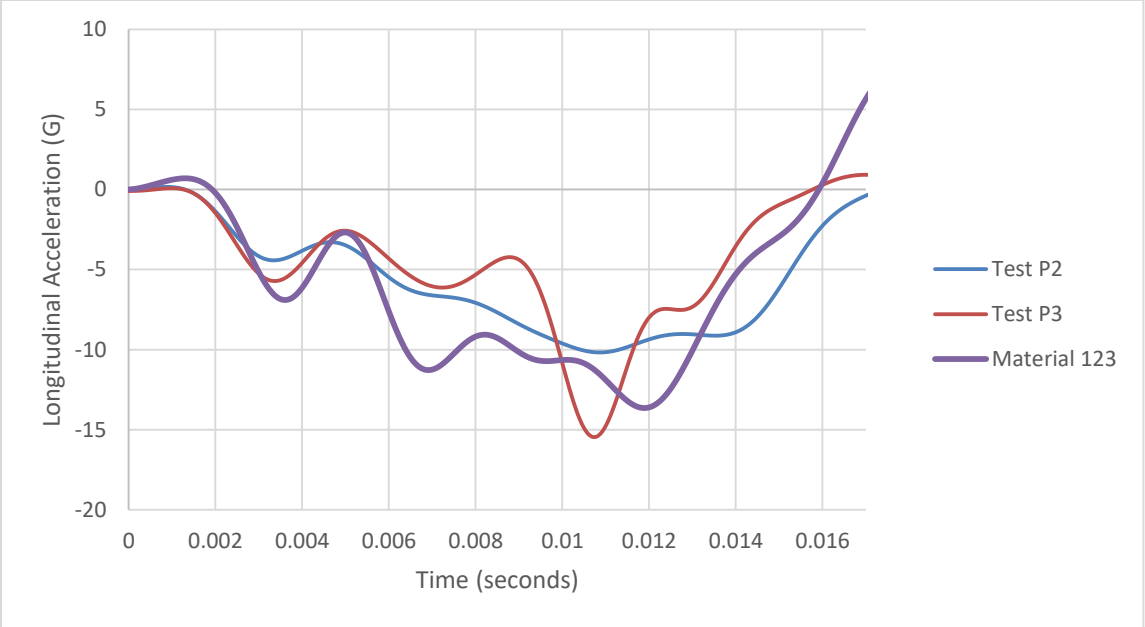

Figure 29. Longitudinal Acceleration for Standard Post in Weak Axis – Material 123

Time: 0.0 seconds

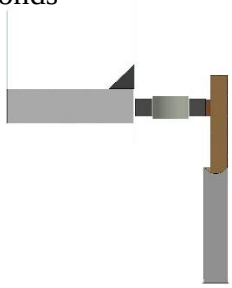

Time: 0.015 seconds

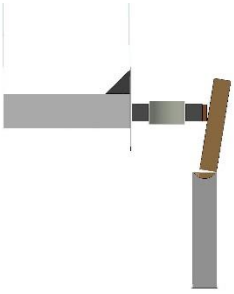

Time: 0.04 seconds

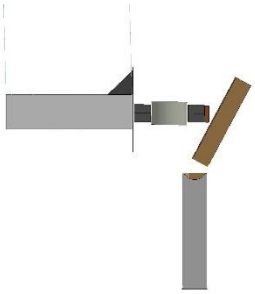

Time: 0.07 seconds

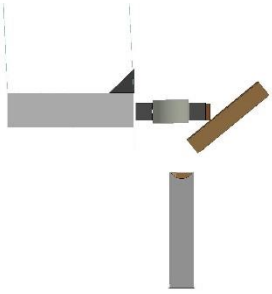

Figure 30. Sequential Images of Standard Post - Weak Axis (143 Wood)

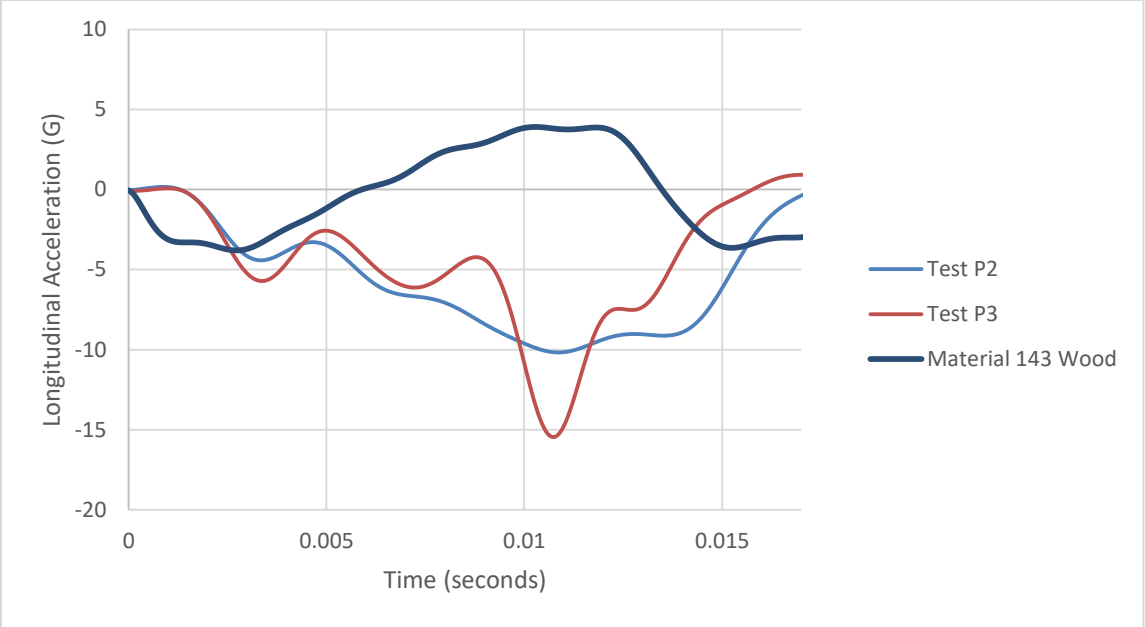

Figure 31. Longitudinal Acceleration for Standard Post in Weak Axis – Material 143 Wood

Time = 0.0 seconds

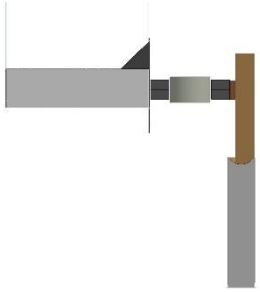

Time = 0.015 seconds

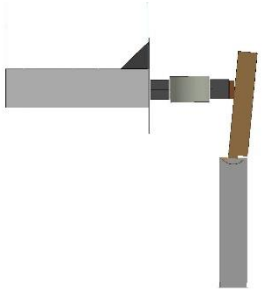

Time = 0.03 seconds

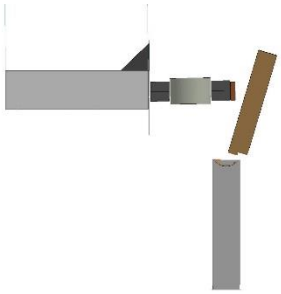

Time = 0.045 seconds

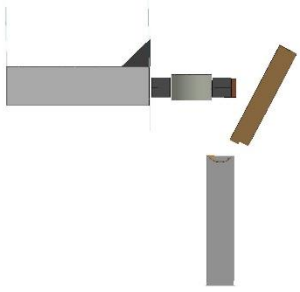

Figure 32. Sequential Images of Standard Post – Weak Axis (143 Wood Pine)

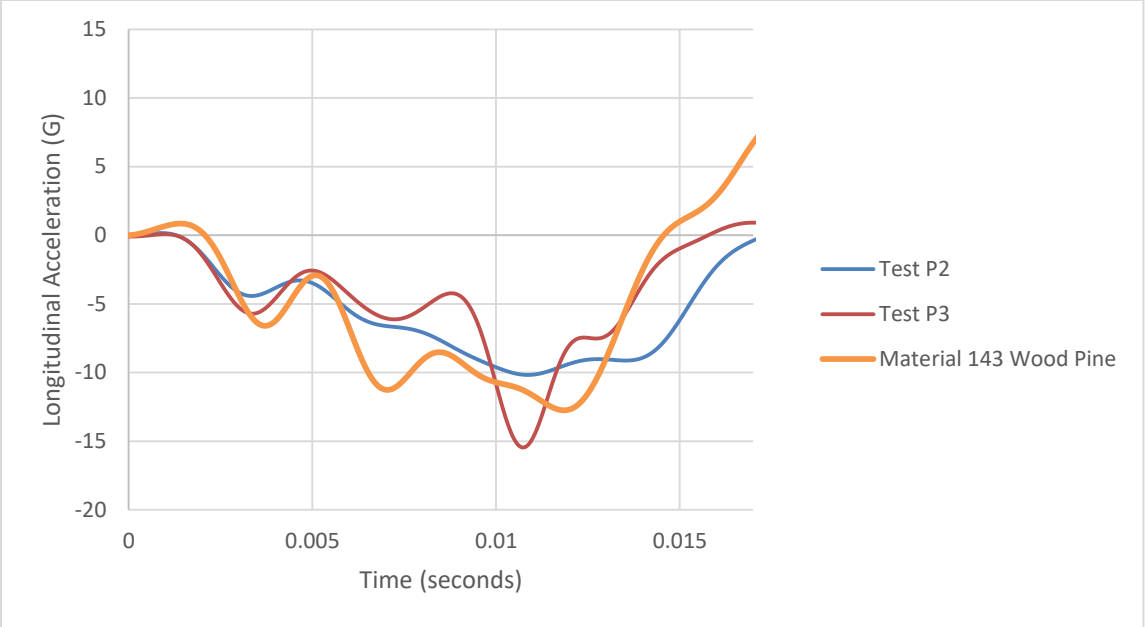

Figure 33. Longitudinal Acceleration for Standard Post in Weak Axis – Material 143 Wood Pine

APPENDIX B

TABLES

Table 1. Material Model 123 - Parameters for Southern Yellow Pine Wood

Material Parameters for Southern Pine Wood	
RO-Density, ton/mm^3	6.63E-10
E-Young Modulus, MPa	11750
PR-Poisson's Ratio	0.3
SIGY-Yield Stress, MPa	60
ETAN-Tangent Modulus, MPa	88
EPSMAJ- Major in Plane Strain at Failure	-0.002 to -0.006

Table 2. Material Model 143 Wood - Parameters for CRT Post in the Strong Axis

Density, ton/mm^3	6.63E-10
Stiffness:	
E_L: Parallel Normal Modulus, MPa	14904
E_T : Perpendicular Normal Modulus, MPa	820.46
G_{LT}: Parallel Shear Modulus, MPa	779.22
G_{TR} : Perpendicular Shear Modulus, MPa	298.86
P_R: Parallel major Poisson's ratio	0.2437
Strength:	
X_t: Parallel Tensile Strength, MPa	83.22
X_c: Parallel Compressive Strength, MPa	36.92
Y_t: Perpendicular Tensile Strength, MPa	2.57
Y_c: Perpendicular Compressive Strength, MPa	7.10
$S_{\|\|}$: Parallel Shear Strength, MPa	9.58
$S_\perp$: Perpendicular Shear Strength, MPa	11.93
Damage:	
Gf1-Parallel Fracture Energy in Tension, MPa · mm	13.71
Gf2-Parallel Facture Energy in Shear, MPa · mm	60.60
Bfit-Parallel Softening Parameter	30
Dmax-Parallel Maximum Damage	0.9999
Gf1-Perpendicular Fracture Energy in Tension, MPa · mm	0.28
Gf2-Perpendicular Facture Energy in Shear, MPa · mm	1.003
Dfit-Perpendicular Softening Parameter	30
Dmax-Perpendicular Maximum Damage	0.99
Hardening:	
$N_{\|\|}$: Parallel Hardening Initiation	0.5
$C_{\|\|}$: Parallel Hardening Rate	793.0
$N_\perp$: Perpendicular Hardening Initiation	0.4
$C_\perp$: Perpendicular Hardening Rate	198.0

Table 3. Material Model 143 Wood - Parameters for CRT Post in the Weak Axis

Density, ton/mm^3	6.63E-10
Stiffness:	
E_L: Parallel Normal Modulus, MPa	11750
E_T : Perpendicular Normal Modulus, MPa	246.8
G_{LT}: Parallel Shear Modulus, MPa	715.22
G_{TR} : Perpendicular Shear Modulus, MPa	87.51
P_R: Parallel major Poisson's ratio	10.58
Strength:	
X_t: Parallel Tensile Strength, MPa	83.22
X_c: Parallel Compressive Strength, MPa	37.96
Y_t: Perpendicular Tensile Strength, MPa	2.57
Y_c: Perpendicular Compressive Strength, MPa	7.3
$S_{\|\|}$: Parallel Shear Strength, MPa	9.57
$S_\perp$: Perpendicular Shear Strength, MPa	12.26
Damage:	
Gf1-Parallel Fracture Energy in Tension, MPa · mm	16.92
Gf2-Parallel Facture Energy in Shear, MPa · mm	60.60
Bfit-Parallel Softening Parameter	30
Dmax-Parallel Maximum Damage	0.9999
Gf1-Perpendicular Fracture Energy in Tension, MPa · mm	0.28
Gf2-Perpendicular Facture Energy in Shear, MPa · mm	1.003
Dfit-Perpendicular Softening Parameter	30
Dmax-Perpendicular Maximum Damage	0.99
Hardening:	
$N_{\|\|}$: Parallel Hardening Initiation	0.5
$C_{\|\|}$: Parallel Hardening Rate	751
$N_\perp$: Perpendicular Hardening Initiation	0.4
$C_\perp$: Perpendicular Hardening Rate	188

Table 4. Material Model 143 Wood - Parameters for Standard Post in the Strong Axis

Density, ton/mm^3	6.63E-10
Stiffness:	
E_L: Parallel Normal Modulus, MPa	11750
E_T : Perpendicular Normal Modulus, MPa	246.8
G_{LT}: Parallel Shear Modulus, MPa	715.22
G_{TR} : Perpendicular Shear Modulus, MPa	87.51
P_R: Parallel major Poisson's ratio	10.58
Strength:	
X_t: Parallel Tensile Strength, MPa	83.22
X_c: Parallel Compressive Strength, MPa	37.96
Y_t: Perpendicular Tensile Strength, MPa	2.57
Y_c: Perpendicular Compressive Strength, MPa	7.3
$S_{\|\|}$: Parallel Shear Strength, MPa	9.57
$S_\perp$: Perpendicular Shear Strength, MPa	12.26
Damage:	
Gf1-Parallel Fracture Energy in Tension, MPa · mm	16.92
Gf2-Parallel Facture Energy in Shear, MPa · mm	60.60
Bfit-Parallel Softening Parameter	30
Dmax-Parallel Maximum Damage	0.9999
Gf1-Perpendicular Fracture Energy in Tension, MPa · mm	0.28
Gf2-Perpendicular Facture Energy in Shear, MPa · mm	1.003
Dfit-Perpendicular Softening Parameter	30
Dmax-Perpendicular Maximum Damage	0.99
Hardening:	
$N_{\|\|}$: Parallel Hardening Initiation	0.5
$C_{\|\|}$: Parallel Hardening Rate	751
$N_\perp$: Perpendicular Hardening Initiation	0.4
$C_\perp$: Perpendicular Hardening Rate	188

Table 5. Material Model 143 Wood - Parameters for Standard Post in the Weak Axis

Density, ton/mm^3	6.63E-10
Stiffness:	
E_L: Parallel Normal Modulus, MPa	11750
E_T : Perpendicular Normal Modulus, MPa	246.8
G_{LT}: Parallel Shear Modulus, MPa	715.22
G_{TR} : Perpendicular Shear Modulus, MPa	87.51
P_R: Parallel major Poisson's ratio	10.58
Strength:	
X_t: Parallel Tensile Strength, MPa	86.14
X_c: Parallel Compressive Strength, MPa	37.96
Y_t: Perpendicular Tensile Strength, MPa	2.65
Y_c: Perpendicular Compressive Strength, MPa	7.3
$S_{\|\|}$: Parallel Shear Strength, MPa	9.91
$S_\perp$: Perpendicular Shear Strength, MPa	12.26
Damage:	
Gf1-Parallel Fracture Energy in Tension, MPa · mm	17.51
Gf2-Parallel Facture Energy in Shear, MPa · mm	62.7
Bfit-Parallel Softening Parameter	30
Dmax-Parallel Maximum Damage	0.9999
Gf1-Perpendicular Fracture Energy in Tension, MPa · mm	0.28
Gf2-Perpendicular Facture Energy in Shear, MPa · mm	1.003
Dfit-Perpendicular Softening Parameter	30
Dmax-Perpendicular Maximum Damage	0.99
Hardening:	
$N_{\|\|}$: Parallel Hardening Initiation	0.5
$C_{\|\|}$: Parallel Hardening Rate	750
$N_\perp$: Perpendicular Hardening Initiation	0.4
$C_\perp$: Perpendicular Hardening Rate	188

Table 6. Material Model 143 Woodpine - Parameters for Southern Yellow Pine Wood

Material Parameters for Southern Pine Wood Units (ton, mm, s, N, MPA)	
RO-Density, ton/mm^3	6.63E-10
HARD	0.05
IFAIL	1
Moisture	12%
Temperature, °C	20
Tension/Shear Quality Factor	0.40 – 0.47
Compression Quality Factor	0.63 – 0.71
A1	0
A2	0
A3	1
D1	1
D2	0
D3	0

Material Model 143 Wood

Input values for material model 143 depending on the moisture content, 1%, 7%, 12% and 23%. The following changes are based on the moisture content and reduction factors Q_t = 0.47 and Q_c = 0.63.

Table 7. Parameters for Southern Yellow Pine with Moisture Content 1%

Moisture Content 1%	
Density, ton/mm^3	6.63E-10
Stiffness:	
E_L: Parallel Normal Modulus, MPa	16720
E_T : Perpendicular Normal Modulus, MPa	959.7
G_{LT}: Parallel Shear Modulus, MPa	811.9
G_{TR} : Perpendicular Shear Modulus, MPa	349.3
P_R: Parallel major Poisson's ratio	0.3
Strength:	
X_t: Parallel Tensile Strength, MPa	42.59
X_c: Parallel Compressive Strength, MPa	54.76
Y_t: Perpendicular Tensile Strength, MPa	1.47
Y_c: Perpendicular Compressive Strength, MPa	10.31
$S_{\|\|}$: Parallel Shear Strength, MPa	9.35
$S_\perp$: Perpendicular Shear Strength, MPa	13.09
Damage:	
Gf1-Parallel Fracture Energy in Tension, MPa · mm	11.67
Gf2-Parallel Facture Energy in Shear, MPa · mm	28.48
Bfit-Parallel Softening Parameter	30
Dmax-Parallel Maximum Damage	0.9999
Gf1-Perpendicular Fracture Energy in Tension, MPa · mm	0.233
Gf2-Perpendicular Facture Energy in Shear, MPa · mm	0.57
Dfit-Perpendicular Softening Parameter	30
Dmax-Perpendicular Maximum Damage	0.99
Hardening:	
$N_{\|\|}$: Parallel Hardening Initiation	0.5
$C_{\|\|}$: Parallel Hardening Rate	1008
$N_\perp$: Perpendicular Hardening Initiation	0.4
$C_\perp$: Perpendicular Hardening Rate	252

Table 8. Parameters for Southern Yellow Pine with Moisture Content 7%

Moisture Content 7%	
Density, ton/mm^3	6.63E-10
Stiffness:	
E_L: Parallel Normal Modulus, MPa	15559
E_T : Perpendicular Normal Modulus, MPa	926.63
G_{LT}: Parallel Shear Modulus, MPa	797.2
G_{TR} : Perpendicular Shear Modulus, MPa	338
P_R: Parallel major Poisson's ratio	0.274
Strength:	
X_t: Parallel Tensile Strength, MPa	63.92
X_c: Parallel Compressive Strength, MPa	42.084
Y_t: Perpendicular Tensile Strength, MPa	2.002
Y_c: Perpendicular Compressive Strength, MPa	8.19
$S_{\|\|}$: Parallel Shear Strength, MPa	9.024
$S_\perp$: Perpendicular Shear Strength, MPa	12.096
Damage:	
Gf1-Parallel Fracture Energy in Tension, MPa · mm	11.31
Gf2-Parallel Facture Energy in Shear, MPa · mm	47.08
Bfit-Parallel Softening Parameter	30
Dmax-Parallel Maximum Damage	0.9999
Gf1-Perpendicular Fracture Energy in Tension, MPa · mm	0.227
Gf2-Perpendicular Facture Energy in Shear, MPa · mm	0.945
Dfit-Perpendicular Softening Parameter	30
Dmax-Perpendicular Maximum Damage	0.99
Hardening:	
$N_{\|\|}$: Parallel Hardening Initiation	0.5
$C_{\|\|}$: Parallel Hardening Rate	1008
$N_\perp$: Perpendicular Hardening Initiation	0.4
$C_\perp$: Perpendicular Hardening Rate	252

Table 9. Parameters for Southern Yellow Pine with Moisture Content 12%

Moisture Content 12%	
Density, ton/mm^3	6.63E-10
Stiffness:	
E_L: Parallel Normal Modulus, MPa	14904
E_T : Perpendicular Normal Modulus, MPa	820.46
G_{LT}: Parallel Shear Modulus, MPa	779.22
G_{TR} : Perpendicular Shear Modulus, MPa	298.86
P_R: Parallel major Poisson's ratio	0.244
Strength:	
X_t: Parallel Tensile Strength, MPa	68.62
X_c: Parallel Compressive Strength, MPa	32.76
Y_t: Perpendicular Tensile Strength, MPa	2.115
Y_c: Perpendicular Compressive Strength, MPa	6.3
$S_{\|\|}$: Parallel Shear Strength, MPa	7.896
$S_\perp$: Perpendicular Shear Strength, MPa	10.584
Damage:	
Gf1-Parallel Fracture Energy in Tension, MPa · mm	11.309
Gf2-Parallel Facture Energy in Shear, MPa · mm	49.97
Bfit-Parallel Softening Parameter	30
Dmax-Parallel Maximum Damage	0.9999
Gf1-Perpendicular Fracture Energy in Tension, MPa · mm	0.227
Gf2-Perpendicular Facture Energy in Shear, MPa · mm	1.00
Dfit-Perpendicular Softening Parameter	30
Dmax-Perpendicular Maximum Damage	0.99
Hardening:	
$N_{\|\|}$: Parallel Hardening Initiation	0.5
$C_{\|\|}$: Parallel Hardening Rate	1008
$N_\perp$: Perpendicular Hardening Initiation	0.4
$C_\perp$: Perpendicular Hardening Rate	252

Table 10. Parameters for Southern Yellow Pine with Moisture Content 23%, at Saturation

Moisture Content 23%	
Density, ton/mm^3	6.63E-10
Stiffness:	
E_L: Parallel Normal Modulus, MPa	11350
E_T : Perpendicular Normal Modulus, MPa	247
G_{LT}: Parallel Shear Modulus, MPa	715
G_{TR} : Perpendicular Shear Modulus, MPa	87.51
P_R: Parallel major Poisson's ratio	0.165
Strength:	
X_t: Parallel Tensile Strength, MPa	47.47
X_c: Parallel Compressive Strength, MPa	13.55
Y_t: Perpendicular Tensile Strength, MPa	0.874
Y_c: Perpendicular Compressive Strength, MPa	2.52
$S_{\|\|}$: Parallel Shear Strength, MPa	4.183
$S_\perp$: Perpendicular Shear Strength, MPa	5.61
Damage:	
Gf1-Parallel Fracture Energy in Tension, MPa · mm	10.46
Gf2-Parallel Facture Energy in Shear, MPa · mm	39.26
Bfit-Parallel Softening Parameter	30
Dmax-Parallel Maximum Damage	0.9999
Gf1-Perpendicular Fracture Energy in Tension, MPa · mm	0.21
Gf2-Perpendicular Facture Energy in Shear, MPa · mm	0.788
Dfit-Perpendicular Softening Parameter	30
Dmax-Perpendicular Maximum Damage	0.99
Hardening:	
$N_{\|\|}$: Parallel Hardening Initiation	0.5
$C_{\|\|}$: Parallel Hardening Rate	1008
$N_\perp$: Perpendicular Hardening Initiation	0.4
$C_\perp$: Perpendicular Hardening Rate	252